

Genetically Adjusted PSA Levels for Prostate Cancer Screening

Linda Kachuri^{1,2,3}, Thomas J. Hoffmann^{1,4}, Yu Jiang², Sonja I. Berndt⁵, John P. Shelley⁶, Kerry Schaffer⁷, Mitchell J. Machiela⁵, Neal D. Freedman⁵, Wen-Yi Huang⁵, Shengchao A. Li⁵, Ryder Easterlin⁸, Phyllis J. Goodman⁹, Cathee Till¹⁰, Ian Thompson¹¹, Hans Lilja^{12,13}, Stephen K. Van Den Eeden¹⁴, Stephen J. Chanock⁵, Christopher A. Haiman^{15,16}, David V. Conti^{15,16}, Robert J. Klein¹⁷, Jonathan D. Mosley^{6,18}, Rebecca E. Graff^{1*}, John S. Witte^{1,2,3,19*}

Affiliations:

1. Department of Epidemiology & Biostatistics, University of California San Francisco, San Francisco, CA, USA
2. Department of Epidemiology & Population Health, Stanford University School of Medicine, Stanford, CA, USA
3. Stanford Cancer Institute, Stanford University School of Medicine, Stanford, CA, USA
4. Institute of Human Genetics, University of California San Francisco, San Francisco, CA, USA
5. Division of Cancer Epidemiology and Genetics, National Cancer Institute, Rockville, MD, USA
6. Department of Biomedical Informatics, Vanderbilt University Medical Center, Nashville, TN, USA
7. Division of Hematology and Oncology, Vanderbilt University Medical Center, Nashville, TN, USA
8. Biological and Medical Informatics, University of California San Francisco, San Francisco, CA, USA
9. Fred Hutchinson Cancer Research Center, Seattle, WA, USA
10. SWOG Statistics and Data Management Center, Fred Hutchinson Cancer Research Center, Seattle, WA, USA
11. CHRISTUS Santa Rosa Medical Center Hospital, San Antonio, TX, USA
12. Departments of Laboratory Medicine, Surgery, Medicine, Memorial Sloan Kettering Cancer Center, New York, NY, USA
13. Department of Translational Medicine, Lund University, Skåne University Hospital, Malmö, Sweden
14. Division of Research, Kaiser Permanente Northern California, Oakland, CA, USA
15. Center for Genetic Epidemiology, Department of Population and Preventive Health Sciences, Keck School of Medicine, University of Southern California, Los Angeles, CA, USA
16. Norris Comprehensive Cancer Center, Keck School of Medicine, University of Southern California, Los Angeles, CA, USA
17. Department of Genetics and Genomic Sciences, Icahn School of Medicine at Mount Sinai, New York, NY, USA
18. Department of Internal Medicine, Vanderbilt University Medical Center, Nashville, TN, USA
19. Departments of Biomedical Data Science and Genetics (by courtesy), Stanford University, Stanford, CA, USA

* These authors jointly supervised this work

Rebecca E. Graff

Department of Epidemiology and Biostatistics

Mission Hall: Global Health & Clinical Sciences Building

550 16th Street, 2nd Floor, Box #0560

San Francisco, CA 94158

Email: Rebecca.Graff@ucsf.edu

John S. Witte

Department of Epidemiology and Population Health

Alway Building, Suite M121

300 Pasteur Drive

Stanford, CA 94305

Email: jswitte@stanford.edu

ABSTRACT

Prostate-specific antigen (PSA) screening for prostate cancer remains controversial because it increases overdiagnosis and overtreatment of clinically insignificant tumors. Accounting for genetic determinants of constitutive, non-cancer-related PSA variation has potential to improve screening utility. We discovered 128 genome-wide significant associations ($P < 5 \times 10^{-8}$) in a multi-ancestry meta-analysis of 95,768 men and developed a PSA polygenic score (PGS_{PSA}) that explains 9.61% of constitutive PSA variation. We found that in men of European ancestry, using PGS-adjusted PSA would avoid 31% of negative prostate biopsies, but also result in 12% fewer biopsies in patients with prostate cancer, mostly with Gleason score < 7 tumors. Genetically adjusted PSA was more predictive of aggressive prostate cancer (odds ratio (OR)=3.44, $P=6.2 \times 10^{-14}$; AUC=0.755) than unadjusted PSA (OR=3.31, $P=1.1 \times 10^{-12}$; AUC=0.738) in 106 cases and 23,667 controls. Compared to a prostate cancer PGS alone (AUC=0.712), including genetically adjusted PSA improved detection of aggressive disease (AUC=0.786, $P=7.2 \times 10^{-4}$). Our findings highlight the potential utility of incorporating PGS for personalized biomarkers in prostate cancer screening.

MAIN

Prostate-specific antigen (PSA) is an enzyme produced by the prostate gland, which degrades gel-forming seminal proteins to release of motile sperm and is encoded by the kallikrein-3 (*KLK3*) gene¹⁻³. As prostate epithelial tissue becomes disrupted by a tumor, greater PSA concentrations are released into circulation^{2,3}. PSA levels can also rise due to prostatic inflammation, infection, benign prostatic hyperplasia, older age, and increased prostate volume³⁻⁵. Increased body mass index is associated with lower PSA levels, but the underlying mechanisms remain unclear^{6,7}. Low PSA levels thus do not rule out prostate cancer and PSA elevation is not sufficient for a conclusive diagnosis⁸. Although PSA testing reduces deaths from prostate cancer⁹, between 20 and 60% of cancers detected using PSA testing are estimated to be overdiagnoses¹⁰⁻¹². In addition, the long-term risk of lethal prostate cancer remains low, especially in men with PSA below the age-specific median^{13,14}. As a result, clinical guidelines in the United States and globally advise against population-level PSA screening and promote a shared decision-making model^{15,16}.

One avenue for refining PSA screening is by accounting for variability in PSA due to genetic factors. PSA is highly heritable, with 40 independent loci identified in the largest previous genome-wide association study (GWAS)^{17,18}. The goal of genetically correcting PSA levels is to increase the relative variation in PSA attributable to prostate cancer, thereby improving their predictive value for disease detection. The first study to genetically correct PSA using just four variants reclassified 3% of participants to warranting biopsy and 3% to avoiding biopsy¹⁹. Incorporating additional genetic predictors has the potential to personalize PSA testing, reduce overdiagnosis-related morbidity, and improve detection of lethal disease. To maximize the utility of this approach, it is critical to distinguish genetic variants that influence constitutive PSA levels from those affecting prostate tumor development. PSA and prostate cancer share many genetic loci^{17,19-22}, but the extent to which this overlap reflects screening bias remains unclear, as GWAS of prostate cancer may capture signals for disease susceptibility and incidental detection due to benign PSA elevation.

Our study explores the genetic architecture of PSA levels in men without prostate cancer, with a view toward assessing whether genetic adjustment of PSA improves clinical decision-making related to prostate cancer diagnosis. It also provides a novel framework for the clinical translation of polygenic scores (PGS) for non-causal cancer biomarkers.

RESULTS

The study design of the Precision PSA study is illustrated in **Figure 1**. Using data from five studies (**Methods**), we conducted genome-wide analyses of PSA levels ≤ 10 ng/mL in cis-gender men never diagnosed with prostate cancer. GWAS results were meta-analyzed within ancestry groups and then combined across populations for a total sample size of 95,768 individuals.

Genetic Architecture of PSA Variation

The heritability (h^2) of PSA levels was investigated using several methods to assess sensitivity to underlying modeling assumptions (**Methods**). Across 26,491 men of European ancestry in the UK Biobank (UKB) with linked clinical records, the median PSA value was 2.35 ng/mL (**Supplementary Fig. 1**). Using individual-level data for variants with minor allele frequency (MAF) ≥ 0.01 and imputation INFO >0.80 , PSA heritability was $h^2=0.41$ (95% CI: 0.36-0.46) based on GCTA²³ and $h^2=0.30$ (95% CI: 0.26-0.33) based on LDAK²⁴ (**Supplementary Table 1; Extended Data Fig. 1**). Applying LDAK to GWAS summary statistics generated from the same individuals produced similar estimates ($h^2=0.35$, 0.28-0.43), whereas other methods^{25,26} were biased downward. In the European ancestry GWAS meta-analysis ($N_{EUR}=85,824$), LDAK estimated $h^2=0.30$ (95% 0.29-0.31). Sample sizes for other ancestries were too small for reliable heritability estimates.

The multi-ancestry meta-analysis of 95,768 men from five studies identified 128 independent index variants ($P<5.0\times 10^{-8}$, linkage disequilibrium (LD) $r^2<0.01$ within ± 10 Mb windows) across 90 chromosomal cytoband regions (**Figure 2**). The strongest associations were in known PSA loci^{17,19,21,22}, such as *KLK3* (rs17632542, $P=3.2\times 10^{-638}$), 10q26.12 (rs10886902, $P=8.2\times 10^{-118}$), *MSMB* (rs10993994, $P=7.3\times 10^{-87}$), *NKX3-1* (rs1160267, $P=6.3\times 10^{-83}$), *CLPTM1L* (rs401681, $P=7.0\times 10^{-54}$), and *HNF1B* (rs10908278, $P=2.1\times 10^{-46}$). Eighty-two index variants were independent of previously detected associations in the Genetic Epidemiology Research on Adult

Health and Aging (GERA) cohort¹⁷; they mapped to 56 cytobands where PSA signals have not previously been reported. Associations initially detected in the UKB (**Extended Data Fig. 1b**) strengthened in the meta-analysis: *TEX11* in Xq13.1 (rs62608084, $P=1.7\times 10^{-24}$); *THADA* in 2p21 (rs11899863, $P=1.7\times 10^{-13}$); *OTX1* in 2p15 (rs58235267, $P=4.9\times 10^{-13}$); *SALL3* in 18q23 (rs71279357, $P=1.8\times 10^{-12}$); and *ST6GAL1* in 3q27.3 (rs12629450, $P=2.6\times 10^{-10}$). Additional novel findings included *CDK5RAP1* (rs291671, $P=1.2\times 10^{-18}$), *LDAH* (rs10193919, $P=1.5\times 10^{-15}$), *ABCC4* (rs61965887, $P=3.7\times 10^{-14}$), *INKA2* (rs2076591, $P=2.6\times 10^{-13}$), *SUDS3* (rs1045542, $P=1.2\times 10^{-13}$), *FAF1* (rs12569177, $P=3.2\times 10^{-13}$), *JARID2* (rs926309, $P=1.6\times 10^{-12}$), *GPC3* (rs4829762, $P=5.9\times 10^{-12}$), *EDA* (rs2520386, $P=4.2\times 10^{-11}$), and *ODF3* (rs7103852, $P=1.2\times 10^{-9}$) (**Supplementary Tables 2-3**).

Of the 128 index variants, 96 reached genome-wide significance in the European ancestry meta-analysis, as did three in the East Asian ancestry meta-analysis (*KLK3*: rs2735837, rs374546878; *MSMB*: rs10993994; $N_{EAS}=3,337$), two in the Hispanic/Latino meta-analysis (*KLK3*: rs17632542, rs2735837; $N_{HIS/LAT}=3,098$), and one (*FGFR2*: rs10749415; $N_{AFR}=3,509$) in the African ancestry meta-analysis (**Supplementary Table 4**). Effect sizes from the European ancestry GWAS were modestly correlated with estimates from other ancestries (Spearman's $\rho_{HIS/LAT}=0.48$, $P=1.1\times 10^{-8}$; $\rho_{AFR}=0.27$, $P=2.0\times 10^{-3}$; $\rho_{EAS}=0.16$, $P=0.068$) (**Supplementary Fig. 2**). However, cross-population comparisons of correlations should be interpreted with caution as they are confounded by higher sampling error in groups with smaller sample sizes.

There was heterogeneity (Cochran's Q $P_Q<0.05$) across ancestry-specific fixed-effects meta-analyses for 12 out of 128 index variants, four of which had effects in different directions: rs58235267 (*OTX1*), rs1054713 (*KLK1*), rs10250340 (*EIF4HP1*), and rs7020681 (*SLC35D2*) (**Supplementary Table 5**). An alternative meta-analysis approach, MR-MEGA²⁷, which partitions effect size heterogeneity into components correlated with ancestry and residual variation, identified one additional signal in 5q15 (rs291812, $P_{MR-MEGA}=1.0\times 10^{-8}$) that was driven by East Asian ancestry ($P_{EAS}=1.2\times 10^{-6}$; **Supplementary Table 6**).

Predicted functional consequences of the 128 index variants were explored using CADD²⁸ scores >13 (corresponding to the 5% most deleterious substitutions) were observed for 16 out of the 128 index variants detected with the original approach, including 10 new signals: rs10193919 (*LDAH*); rs7732515 in 5q14.3; rs11899863 (*THADA*); rs58235267 (*OTX1*); rs926309 (*JARID2*); rs4829762 (*GPC3*), rs13268, a missense variant in *FBLN1*; rs78378222 in *TP53*, rs3760230 in *SMG6*; and rs712329 in *SLC25A21* (**Supplementary Table 7**). Sixty-one variants had significant ($FDR<0.05$) effects on gene expression, including 15 prostate tissue eQTLs for 17 eGenes, 55 blood eQTLs for 185 eGenes, and 9 eQTLs with effects in both tissues. Notable eGenes included *RUVBL1*, a chromatin-remodeling factor that modulates pro-inflammatory NF- κ B signaling and transcription of *Myc* and β -catenin²⁹; *ODF3*, which maintains elastic structures in the sperm tail³⁰; and *LDAH*, which promotes cholesterol mobilization in macrophages³¹. Several PSA-associated variants were eQTLs for genes involved in immune response (*IFITM2*, *IFITM3*, *HS1BP3*).

Impact of PSA-Related Selection Bias on Prostate Cancer GWAS

Since prostate cancer detection often hinges on PSA elevation, genetic factors resulting in higher constitutive PSA levels may appear to increase prostate cancer risk because of more frequent screening. Of the 128 lead PSA variants, 52 (41%) were associated with prostate cancer at the Bonferroni-corrected threshold ($p<0.05/128$) in the PRACTICAL consortium's European ancestry GWAS³² (**Supplementary Table 8**). Using the method by Dudbridge et al.³³, we investigated whether index event bias could partly explain these shared signals^{33,34} (**Methods; Figure 3; Supplementary Table 9**). Applying the estimated bias correction factor ($b=1.144$) decreased the number of variants associated with prostate cancer from 52 to 34 (**Extended Data Fig. 2**). When we corrected 209 European ancestry prostate cancer risk variants ($P<5.0\times 10^{-8}$; $LD\ r^2<0.01$) for screening bias, 93 (45%) remained genome-wide significant. Notably, rs76765083 (*KLK3*) remained genome-wide significant, but reversed direction. Sensitivity analyses using SlopeHunter³⁵ resulted in 150 (72%) variants with $P<5\times 10^{-8}$ (**Supplementary Table 10**).

Development and Validation of PGS_{PSA}

We considered two approaches for constructing a PGS for PSA: clumping genome-wide significant associations from the multi-ancestry meta-analysis (PGS₁₂₈) and a genome-wide score generated using the Bayesian PRS-CSx algorithm (PGS_{CSx})³⁶ (**Methods**). Each score was validated in the Prostate Cancer Prevention Trial (PCPT) and Selenium and Vitamin E Cancer Prevention Trial (SELECT), which were excluded from the discovery GWAS. Most of the men in both cohorts were of European ancestry, although SELECT offered larger sample sizes for other ancestry groups (**Extended Data Fig. 3**). PGS_{CSx} was ultimately selected, as it was more predictive of baseline PSA than PGS₁₂₈ in multi-ancestry analyses and most ancestry subgroups (**Supplementary Table 11**).

In PCPT, PGS_{CSx} accounted for 8.13% of variation in baseline PSA levels (β per SD increase = 0.186, $P=3.3\times 10^{-112}$) in the pooled multi-ancestry sample of 5883 men (**Fig. 4a-c; Supplementary Table 11**). PGS_{CSx} was associated with PSA across age groups, although effects attenuated in participants aged ≥ 70 (**Extended Data Fig. 4**). PGS_{CSx} was validated in 5725 participants of European (EUR ≥ 0.80) ancestry (PGS_{CSx}: $\beta=0.194$, $P=1.7\times 10^{-115}$), but neither PGS₁₂₈ nor PGS_{CSx} reached nominal significance in the admixed European and African ancestry ($0.20 < \text{AFR}/\text{EUR} < 0.80$; $n=103$) or East Asian ancestry (EAS ≥ 0.80 ; $n=55$) populations.

In SELECT, PGS_{CSx} was associated with baseline PSA levels in the pooled sample of 25,917 men ($\beta=0.258$, $P=1.3\times 10^{-619}$) and among men of European ancestry ($\beta_{\text{PGS}}=0.283$, $P=5.5\times 10^{-610}$; $n=22,253$), accounting for 9.61% to 10.94% of variation, respectively (**Fig. 4b-d; Supplementary Table 11**). PGS_{CSx} also validated in the East Asian ($n=257$) ($\beta=0.258$, $P=5.9\times 10^{-7}$) and admixed EAS/EUR ($n=321$; $\beta=0.315$, $P=5.2\times 10^{-12}$) ancestry groups. In men with admixed AFR/EUR ancestry ($n=1763$), PGS_{CSx} explained 4.22% of PSA variation ($\beta=0.157$, $P=4.8\times 10^{-19}$). PGS₁₂₈ was more predictive than PGS_{CSx} ($\beta=0.163$, $P=8.2\times 10^{-11}$ vs. $\beta=0.098$, $P=8.0\times 10^{-6}$) in men of African ancestry (AFR ≥ 0.80 ; $n=1173$) and the pooled AFR and admixed ($0.20 < \text{EUR}/\text{AFR} < 0.80$) group ($n=2936$).

We also examined associations with temporal trends in PSA: velocity, calculated using $\log(\text{PSA})$ values at two time points, and doubling time in months (**Methods; Supplementary Table 12**). In men with a PSA increase (SELECT pooled sample: $n=14,908$), PGS_{CSx} was associated with less rapid velocity (PGS_{CSx}: $\beta=-4.06\times 10^{-4}$, $P=3.7\times 10^{-5}$;) and longer doubling time (PGS_{CSx}: $\beta=10.41$, $P=1.9\times 10^{-8}$). In men with a PSA decrease between the first and last time point (SELECT pooled sample: $n=6970$), PGS_{CSx} was only suggestively associated with slowing PSA decline ($\beta=5.02\times 10^{-4}$, $P=0.068$). The same pattern was observed in PCPT, with higher PGS_{CSx} values conferring less rapid changes in PSA.

PGS_{CSx}, referred to as PGS_{PSA} from here onward, was used to genetically adjust baseline or earliest pre-randomization PSA values (PSA^G) for each individual, relative to the population mean (**Methods, Equations 1-2**). PSA^G and unadjusted PSA were strongly correlated in PCPT (Pearson's $r=0.841$, $0.833-0.848$) and SELECT ($r=0.854$, $0.851-0.857$). The number of participants with PSA^G >4 ng/mL, a commonly used threshold for diagnostic testing, increased from 0 to 24 in PCPT and 5 to 413 in SELECT (**Fig. 4e-f**), reflecting the preferential trial selection of men with low PSA^{8,37}.

Impact of PSA-Related Bias on PGS Associations

In men of European ancestry UKB excluded from the PSA GWAS, there was a strong positive relationship between the 269-variant prostate cancer PGS (PGS₂₆₉)³² and PGS_{PSA} in cases ($\beta=0.190$, $P=2.3\times 10^{-96}$; $n=11,568$) and controls ($\beta=0.236$, $P<10^{-700}$; $n=152,884$) (**Extended Data Fig. 5, Supplementary Table 13**). Refitting PGS₂₆₉ using weights corrected for index event bias (PGS₂₆₉^{adj}) substantially attenuated associations in cases ($\beta_{\text{adj}}=0.029$, $P=2.7\times 10^{-3}$) and controls ($\beta_{\text{adj}}=0.052$, $P=2.2\times 10^{-89}$).

To further characterize the impact of this bias, we examined PGS₂₆₉ associations with prostate cancer status in 3673 cases and 2363 biopsy-confirmed, European ancestry controls from GERA. PGS₂₆₉^{adj} had a larger magnitude of association with prostate cancer (OR for top decile=3.63, 95% CI: 3.01-4.37) than PGS₂₆₉ (OR=2.71, 2.28-3.21) and higher area under the curve (AUC: 0.685 vs. 0.677, $P=3.91\times 10^{-3}$) (**Supplementary Table 14**). The impact of bias correction was pronounced for Gleason ≥ 7 tumors (PGS₂₆₉^{adj} AUC=0.692 vs.

PGS₂₆₉ AUC=0.678, $P=1.91 \times 10^{-3}$), although these AUC estimates are inflated due to overlap with the GWAS used to develop PGS₂₆₉³². In case-only analyses, PGS_{PSA} and PGS₂₆₉ were inversely associated with Gleason score, illustrating how screening bias decreases the likelihood of identifying high-grade disease (**Supplementary Table 15**). Compared to Gleason ≤ 6 tumors, an SD increase in PGS_{PSA} was inversely associated with Gleason 7 (OR=0.79, 0.76-0.83) and Gleason ≥ 8 disease (OR=0.71, 0.64-0.81). Patients in the top decile of PGS₂₆₉ were approximately 30% less likely to have Gleason ≥ 8 (OR=0.72, 0.54-0.96) than Gleason ≤ 6 tumors, but this association was attenuated after bias correction (PGS₂₆₉^{adj}: OR=0.94, 0.75-1.17).

Impact of Genetic Adjustment of PSA on Biopsy Eligibility

Among GERA participants who underwent prostate biopsy, we examined how adjustment using PGS_{PSA} reclassified individuals for biopsy recommendation at age-specific thresholds used by Kaiser Permanente: 40-49 years old=2.5 ng/ml; 50-59 years old=3.5 ng/ml; 60-69 years old=4.5 ng/ml; and 70-79 years old=6.5 ng/ml (**Methods**). For men of European ancestry, mean PSA levels in men with a negative biopsy (7.2 ng/mL, n=2363) were higher than in men without prostate cancer who did not have a biopsy (1.5 ng/mL; n=24,811) (**Supplementary Table 16**). Relative to all controls, where standardized $\overline{PGS}_{PSA} = 0$, biopsied men were enriched for PSA-increasing alleles (cases: $\overline{PGS}_{PSA} = 0.278$; controls: $\overline{PGS}_{PSA} = 0.934$). After genetic adjustment, 31.7% of biopsy-negative men were reclassified below the PSA level for recommending biopsy, and 2.5% became biopsy-eligible, resulting in a net reclassification of 29.3% (27.5% to 31.21%) (**Fig. 5a**). Among 3673 cases PSA^G values below the biopsy referral threshold were more prevalent than upward adjustment, resulting in a net reclassification of -8.6% (-9.48% to -7.67%) (**Fig. 5a**). Of the patients who became ineligible, most had Gleason < 7 tumors (n=300, 72%; **Supplementary Table 16**). In men of African ancestry, there were few changes in biopsy eligibility among cases (n=392), with 3.1% reclassified upward and 4.6% downward (**Fig. 5b**; **Supplementary Table 16**). Of 108 biopsy-negative controls, 75 (69.4%) were reclassified below the referral threshold based on PSA^G, reflecting high enrichment for predisposition to PSA elevation ($\overline{PGS}_{PSA} = 1.710$). The overall net reclassification was positive, suggesting that PSA^G has some clinical utility in both populations.

PSA Genetic Adjustment Improves Prostate Cancer Detection

The utility of PSA^G, alone and in combination with PGS₂₆₉, was first assessed in PCPT, where end-of-study biopsies were performed in all participants, effectively eliminating potential misclassification of prostate cancer status. Among 335 cases and 5548 controls, PGS_{PSA} was not associated with prostate cancer incidence (pooled: OR per SD=1.01, $P=0.83$), confirming it captures genetic determinants of non-cancer PSA variation. The magnitude of association for genetically adjusted baseline PSA^G with prostate cancer (OR per unit increase in log(ng/mL) =1.90, 95% CI: 1.56-2.31) was slightly larger than for PSA (OR=1.88, 1.55-2.29) in the European ancestry group (**Supplementary Table 17**). The magnitude of association with prostate cancer was larger for PGS₂₆₉^{adj} (pooled and European: OR per SD=1.57, 1.40-1.76) than for PGS₂₆₉ without bias correction (pooled: OR=1.52, 1.36-1.70; European: OR=1.53, 1.36-1.72) (**Supplementary Table 17**). The model with PGS₂₆₉^{adj} and PSA^G achieved the best classification in the pooled (AUC=0.686) and European ancestry (AUC=0.688) populations, and outperformed PGS₂₆₉^{adj} alone (pooled: AUC=0.656, $P_{AUC}=7.5 \times 10^{-4}$; European: AUC=0.658, $P_{AUC}=1.4 \times 10^{-3}$).

The benefit of genetically adjusting PSA was most evident for detection of aggressive prostate cancer, defined as Gleason ≥ 7 , PSA ≥ 10 ng/mL, T3-T4 stage, and/or distant or nodal metastases. In PCPT, PSA^G conferred an approximately 3-fold risk increase (pooled: OR=2.87, 1.98-4.65, AUC=0.706; European: OR=2.99, 1.95-4.59, AUC=0.711) compared to PGS₂₆₉^{adj} (pooled: OR=1.55, 1.23-1.95, AUC=0.651; European: OR=1.55, 1.22-1.96, AUC=0.657; **Fig. 6a**; **Supplementary Table 18**). The model with PSA^G and PGS₂₆₉^{adj} achieved AUC=0.726 (European: AUC=0.734) for aggressive tumors, but had lower discrimination for non-aggressive disease (pooled and European: AUC=0.681; **Supplementary Table 19**). Among patients with prostate cancer, PSA^G (pooled: OR=2.06, 1.23-3.45) and baseline PSA (pooled: OR=1.81, 1.12-3.10) were associated with higher likelihood of aggressive compared to non-aggressive tumors, whereas PGS₂₆₉ (pooled: OR=0.91, $P=0.54$) and PGS₂₆₉^{adj} (OR=0.97, $P=0.85$) were not (**Supplementary Table 20**).

In SELECT, associations with risk of prostate cancer overall (**Supplementary Table 21**), aggressive (**Fig. 6b; Supplementary Table 22**), and non-aggressive disease (**Supplementary Table 23**) in the pooled and European ancestry analyses were comparable to PCPT. In men of East Asian ancestry, associations for PSA^G (OR=2.15, 0.82-5.62) were attenuated compared to PSA (OR=2.60, 1.03-6.54). This was also observed in men of African ancestry, although the effect size for PSA^G derived using PGS₁₂₈ (OR=3.37, 2.38-4.78) was larger than for PSA^G based on PGS_{CSx} (OR=2.68, 1.94-3.69), consistent with the larger proportion of variation in PSA explained by PGS₁₂₈ than PGS_{CSx} in this population. Models for prostate cancer including PSA^G were calibrated in the pooled and European ancestry individuals, while in the African ancestry subgroup, PSA^G inaccurately estimated risk in upper deciles (**Supplementary Fig. 3-6**).

The largest improvement in discrimination from PSA^G (OR=3.81, 2.62-5.54; AUC=0.777) relative to PSA (OR=3.40, 2.34-4.93; AUC=0.742, P_{AUC} =0.026) and to PGS₂₆₉ (OR=1.76, 1.41-2.21; AUC=0.726; P_{AUC} =0.057) was for aggressive tumors in men of European ancestry (106 cases, 23,667 controls). In the pooled African ancestry population (18 cases, 2733 controls), PSA^G based on PGS₁₂₈ (OR=2.96, 1.43-6.12), but not PGS_{CSx} (OR=2.48, 1.24-4.97), was more predictive than unadjusted PSA (OR=2.82, 1.33-5.99; **Supplementary Table 22**). The best model for aggressive disease included PSA^G and PGS₂₆₉^{adj} for pooled (AUC=0.788, 95% CI: 0.744-0.831) and European ancestry populations (AUC=0.804, 0.757-0.851), but for African ancestry individuals, unadjusted PSA and PGS₂₆₉ without bias correction achieved the highest AUC of 0.828 (95% CI: 0.739-0.916). PSA^G was better calibrated than PSA in pooled and European ancestry groups, but not in African ancestry participants (**Supplementary Fig. 7-8**).

DISCUSSION

Serum PSA is the most widely used biomarker for prostate cancer detection, although concerns with specificity, and to a lesser degree sensitivity, have limited adoption of PSA testing for population-level screening. Leveraging PGS to personalize diagnostic biomarkers, such as PSA, provides a new avenue for translating GWAS discoveries into clinical practice. This concept, “de-Mendelization,” is essentially Mendelian randomization in reverse – subtracting the genetically-predicted component of trait variance instead of using it to estimate causal effects. De-Mendelization of non-causal predictive biomarkers can maximize disease-related signal and improve disease detection^{38,39}. While previous work on PSA genetics¹⁹ and other biomarkers^{38,40} has alluded to the potential of genetic adjustment to produce clinically meaningful shifts in the PSA distribution, the value of this approach for reducing overdiagnosis and detecting aggressive disease has not been previously shown.

Risk stratified, personalized screening for prostate cancer will require parallel efforts to elucidate the genetic architecture of prostate cancer susceptibility and PSA variation in individuals without disease. Our GWAS advances these efforts by discovering 82 novel PSA-associated variants. The strongest novel signals map to genes involved in reproductive processes, potentially reflecting non-cancer function of PSA in liquefying seminal fluid. *TEX11* on Xq13.1 is preferentially expressed in male germ cells and early spermatocytes. *TEX11* mutations cause meiotic arrest and azoospermia, and this gene regulates homologous chromosome synapsis and double-strand DNA break repair⁴¹. *ODF3* encodes a component of sperm flagella fibers and has been linked to regulation of platelet count and volume⁴². Other novel loci contained genes involved in embryonic development, epigenetic regulation, and chromatin organization, including *DNMT3A*, *OTX1*, *CHD3*, *JARID2*, *HMGA1*, *HMGA2*, and *SUDS3*. *DNMT3A* is a methyltransferase that regulates imprinting and X-chromosome inactivation, and has been studied extensively in the context of height⁴³, clonal hematopoiesis, and hematologic cancers⁴⁴. *CHD3* is involved in chromatin remodeling during development and suppresses herpes simplex virus infection⁴⁵. Multiple PSA-associated variants were in genes related to infection and immunity, including *HLA-A*; *ST6GAL1*, involved in IgG N-glycosylation⁴⁶; *KLRG1*, which regulates NK cell function and IFN- γ production⁴⁷; and *FUT2*, which affects ABO precursor H antigen presentation and confers susceptibility to viral and bacterial infections⁴⁸.

Although our GWAS was restricted to men without prostate cancer, several cancer susceptibility genes were among the PSA-associated loci, including a pan-cancer risk variant in *TP53* (rs78378222)⁴⁹ and signals in *TP63*,

GPC3, and *THADA*. While we cannot rule out undiagnosed prostate cancer in our participants, its prevalence is unlikely to be high enough to produce appreciable bias. Pervasive pleiotropy and omnigenic architecture⁵⁰ may explain the diverse functions of PSA loci implicated in inflammation, epigenetic regulation, and growth factor signaling. Even established tumor suppressor genes, like *TP53*, *GPC3*, and *THADA* have pleiotropic effects on obesity via dysregulation of cell growth and metabolism⁵¹⁻⁵³. Furthermore, distinct p63 isoforms regulate epithelial and craniofacial development, as well as apoptosis of male germ cells and spermatogenesis^{54,55}. Mutations in *GPC3* cause Simson-Golabi-Behmel syndrome, which is characterized by visceral and skeletal abnormalities and excess risk of embryonic tumors⁵⁶.

Distinguishing variants that influence prostate cancer detection via PSA screening from genetic signals for prostate carcinogenesis has implications for deciphering biological mechanisms and developing risk prediction models. Prostate cancer detection depends on PSA testing, while PSA screening is influenced by genetic factors affecting constitutive PSA levels. The bias arising from this complex relationship may be substantial. Our findings suggest that bias-corrected effect sizes more accurately capture the contribution of GWAS-identified variants to prostate cancer risk, without conflating it with detection. Correction for PSA-related bias and subsequent improvement in PGS₂₆₉ performance for detecting aggressive disease is an extension of de-Mendelization. Adjusting risk allele weights may be a more effective strategy than filtering out variants based on associations with PSA. Generally, the improvements in PSA^G and PGS₂₆₉ are proportional to the extent of their de-noising of signals for PSA elevation unrelated to prostate cancer. The impact of bias correction was most pronounced in populations selected for high PSA, such as men who underwent prostate biopsy in GERA, but it was also observed in PCPT and SELECT, which enrolled men with low PSA.

Our investigation of index event bias has several limitations. The Dudbridge method assumes that direct genetic effects on PSA levels and prostate cancer susceptibility are uncorrelated, and violations of this assumption over-attribute shared genetic signals to selection bias³³. Although SlopeHunter relaxes this assumption³⁵, analyses of PGS₂₆₉ suggest it under-corrects selection bias. SlopeHunter relies on clustering to distinguish PSA-specific from pleiotropic variants³⁵, with small or poorly separated clusters resulting in unstable bias estimates. Disentangling genetic associations between PSA and prostate cancer with greater certainty will require experiments, such as CRISPR screens and massively parallel reporter assays.

Another limitation is that the reported magnitude of biopsy reclassification may be specific to GERA and Kaiser Permanente clinical guidelines and biased since GERA controls comprised 30% of the PSA discovery GWAS. Since it was unlikely for men with low PSA to be biopsied and most patients with prostate cancer already had PSA values at or above the biopsy referral cutoff, there were limited opportunities to increase biopsy eligibility in this population. Despite these limitations, our findings indicate that genetically adjusted PSA may reduce overdiagnosis and overtreatment, albeit accompanied by some undesirable loss of sensitivity. While reclassifying cases to not receive biopsy is concerning, most such reclassifications occurred among patients with non-aggressive disease, a group susceptible to overdiagnosis⁵⁷.

Our PGS-based approach updates the first application of PSA genetic correction by Gudmundsson et al.¹⁹ while retaining straightforward calculation of the genetic correction factor. Increasing the specificity of an established, clinically useful biomarker is efficient and would have low adoption barriers. However, analytic choices, such as selecting an optimal PGS algorithm and reference population for obtaining mean PGS_{PSA}, are not trivial. The choice of reference population affects the magnitude of correction and clinical decisions based on absolute PSA values. Furthermore, any new biomarker would require validation in real-world settings to identify populations who would benefit most and characterize barriers to implementation, such as physician familiarity with PGS and patient education about genetic testing. Genetically adjusted PSA should also be evaluated in conjunction with other procedures used for prostate cancer detection, such as targeted MRI, and explored as a criterion for refining selection of participants into screening trials.

Our study highlights the importance and challenge of developing a PGS that adequately performs across the spectrum of ancestry. Compared to PGS₁₂₈, PGS_{CSx} did not improve performance in men of African ancestry. This may reflect the 'meta' estimation procedure, which does not require a separate dataset for hyperparameter tuning, but is less accurate³⁶. GWAS efforts in larger and more diverse cohorts are under way and will expand

the catalog of PSA-associated variants and increase their utility. Genetic adjustment using a PGS_{PSA} that does not explain a sufficiently high proportion of trait variation risks decreasing the accuracy of PSA screening.

Future research should assess whether genetically adjusted PSA levels improve prediction of prostate cancer mortality and investigate PSA-related biomarkers, such as the ratio of free to total PSA and pro-PSA, which may have higher specificity for prostate cancer detection^{58,59}. Although PGS_{PSA} was associated with PSA doubling time and velocity, these metrics assess change between two time points and may not capture PSA trajectories meaningful for disease detection⁶⁰. Clinical guidelines for PSA kinetics are also lacking in the context of prostate cancer screening. Regardless, we believe that genetic adjustment may improve the accuracy of any heritable PSA biomarker and may be a valuable addition to multi-omic biomarkers.

In summary, by detecting genetic variants associated with non-prostate cancer PSA variation, we developed a PGS_{PSA} that captures the contribution of common genetic variants to a man's inherent PSA level. We showed that a straightforward calculation of genetically adjusted, personalized PSA levels using PGS_{PSA} provides clinically meaningful improvements in prostate cancer diagnostic characteristics. Moreover, genetic determinants of PSA provide an avenue for mitigating selection bias due to PSA screening in prostate cancer GWAS and improving disease prediction. These results illustrate a proof of concept for incorporating genetic factors into PSA screening for prostate cancer and expanding this approach to other diagnostic biomarkers.

ACKNOWLEDGEMENTS

The Precision PSA study is supported by funding from the National Institutes of Health (NIH) National Cancer Institute (NCI) under award number R01CA241410 (JSW) and K99CA246076 (LK) and the Young Investigator Award from the Prostate Cancer Foundation (REG). Contributing studies were supported by research grants from the NIH National Institute of General Medical Sciences (NIGMS) under award number R01GM130791 (JDM); NIH/NCI Cancer Center Support Grant to Memorial Sloan Kettering Cancer Center (P30CA008748), MSKCC Specialized Programs of Research Excellence in Prostate Cancer (P50CA92629, HL), Swedish Cancer Society (Cancerfonden 20 1354 PjF, HL), and General Hospital in Malmö Foundation for Combating Cancer. This work was supported in part through the computational resources and staff expertise provided by Scientific Computing at the Icahn School of Medicine at Mount Sinai. Research reported in this paper was supported by the Office of Research Infrastructure of the National Institutes of Health under award number S10OD026880 and NIH/NCI funding (R01CA175491, R01CA244948; RJK).

The content is solely the responsibility of the authors and does not necessarily represent the official views of the National Institutes of Health.

AUTHOR CONTRIBUTIONS

Concept and design: L.K, T.J.H., R.J.K., J.D.M., R.E.G., J.S.W. Acquisition, analysis or interpretation of data: L.K, T.J.H., Y.J., S.I.B., J.P.S, K.S., M.J.M, N.D.F., W.-Y.H., S.A.L, R.E., P.J.G., C.T., I.T., H.L, S. K.V.D.E, S.J.C., C.A.H., D.V.C., R.J.K., J.D.M., R.E.G., J.S.W. Drafting of the manuscript: L.K, T.J.H., R.E.G., J.S.W. Critical revision of the manuscript for important intellectual content: L.K, T.J.H., Y.J., S.I.B., J.P.S, K.S., M.J.M, N.D.F., W.-Y.H., S.A.L, R.E., P.J.G., C.T., I.T., H.L, S. K.V.D.E, S.J.C., C.A.H., D.V.C., R.J.K., J.D.M., R.E.G., J.S.W.

COMPETING INTERESTS

JSW is a non-employee, cofounder of Avail Bio. HL is named on a patent for intact PSA assays and a patent for a statistical method to detect prostate cancer that is licensed to and commercialized by OPKO Health. HL receives royalties from sales of the test and has stock in OPKO Health. All other authors have no competing interests.

Fig. 1: Overview of the Precision PSA study design. Genome-wide association analyses were conducted in men without prostate cancer and meta-analyzed within each population: European ancestry (EUR), African ancestry (AFR), East Asian ancestry (EAS) and Hispanic/Latino (HIS/LAT). Ancestry-stratified results were used to develop a genome-wide PSA genetic score (PGS_{PSA}) comprised of approximately 1.1 million variants and were also combined into a multi-ancestry meta-analysis of 95,768 men. PGS_{PSA} was validated in the Prostate Cancer Prevention Trial (PCPT) and the Selenium and Vitamin E Cancer Prevention Trial (SELECT), and was used to compute genetically adjusted PSA values (PSA^G). We examined how using PSA^G values affects eligibility for prostate biopsy and evaluated associations with incident prostate cancer.

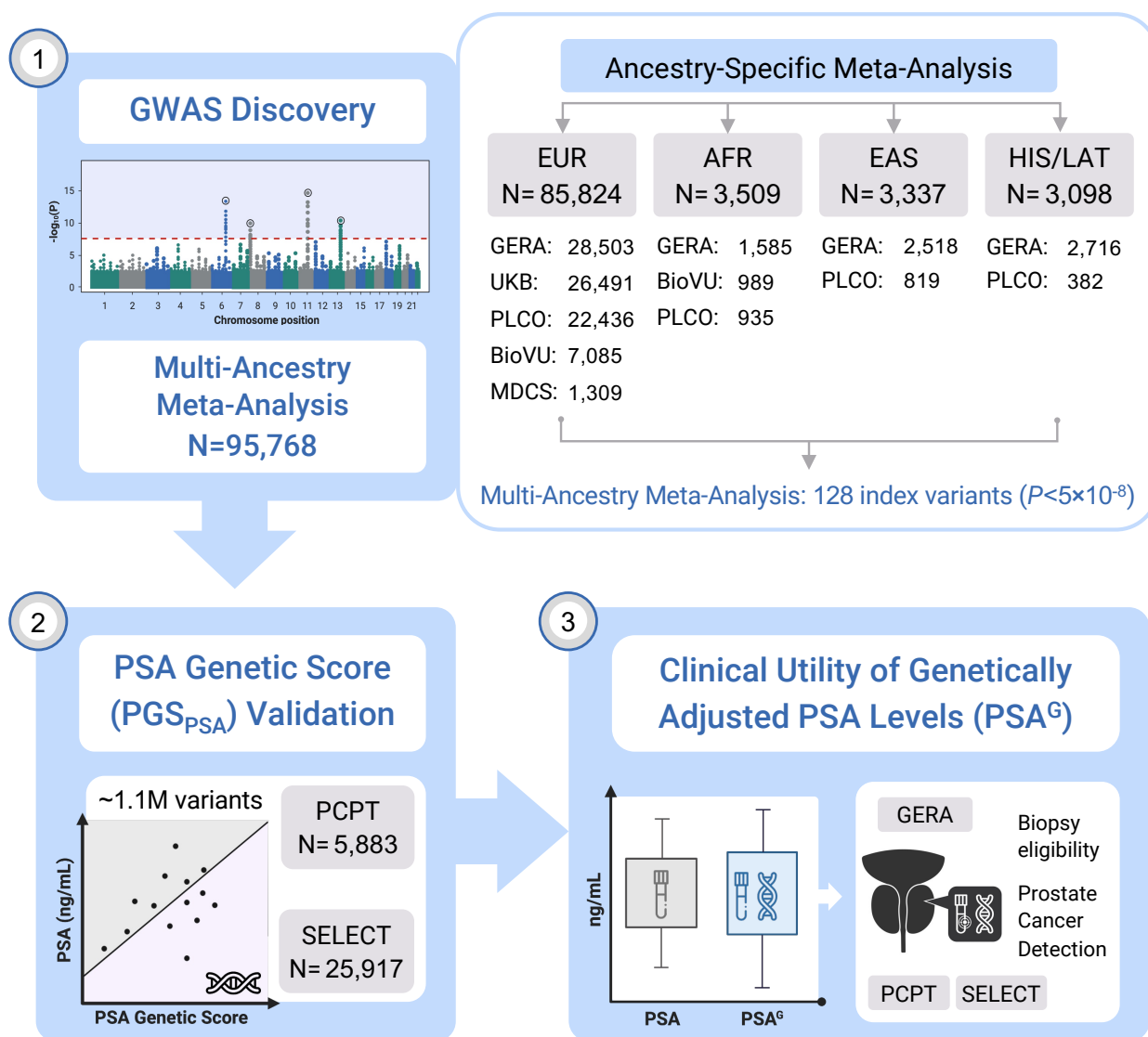


Fig. 2: Multi-ancestry genome-wide association study (GWAS) of PSA levels. **a**, Manhattan plot depicting the results of the GWAS meta-analysis of PSA levels in 95,768 men without prostate cancer. The genome-wide significance threshold of $P < 5 \times 10^{-8}$ is indicated by the dotted black line. Index variants within known PSA-associated loci are annotated with the corresponding cytoband. Novel findings are highlighted in yellow. **b**, Circular dendrogram shows the nearest gene(s) for novel PSA-associated variants. Genome-wide significant ($P < 5 \times 10^{-8}$) index variants were selected using linkage disequilibrium (LD)-based clumping (LD $r^2 < 0.01$ within 10Mb windows). All GWAS p-values are two-sided and derived from a fixed-effects inverse-variance-weighted meta-analysis using METAL.

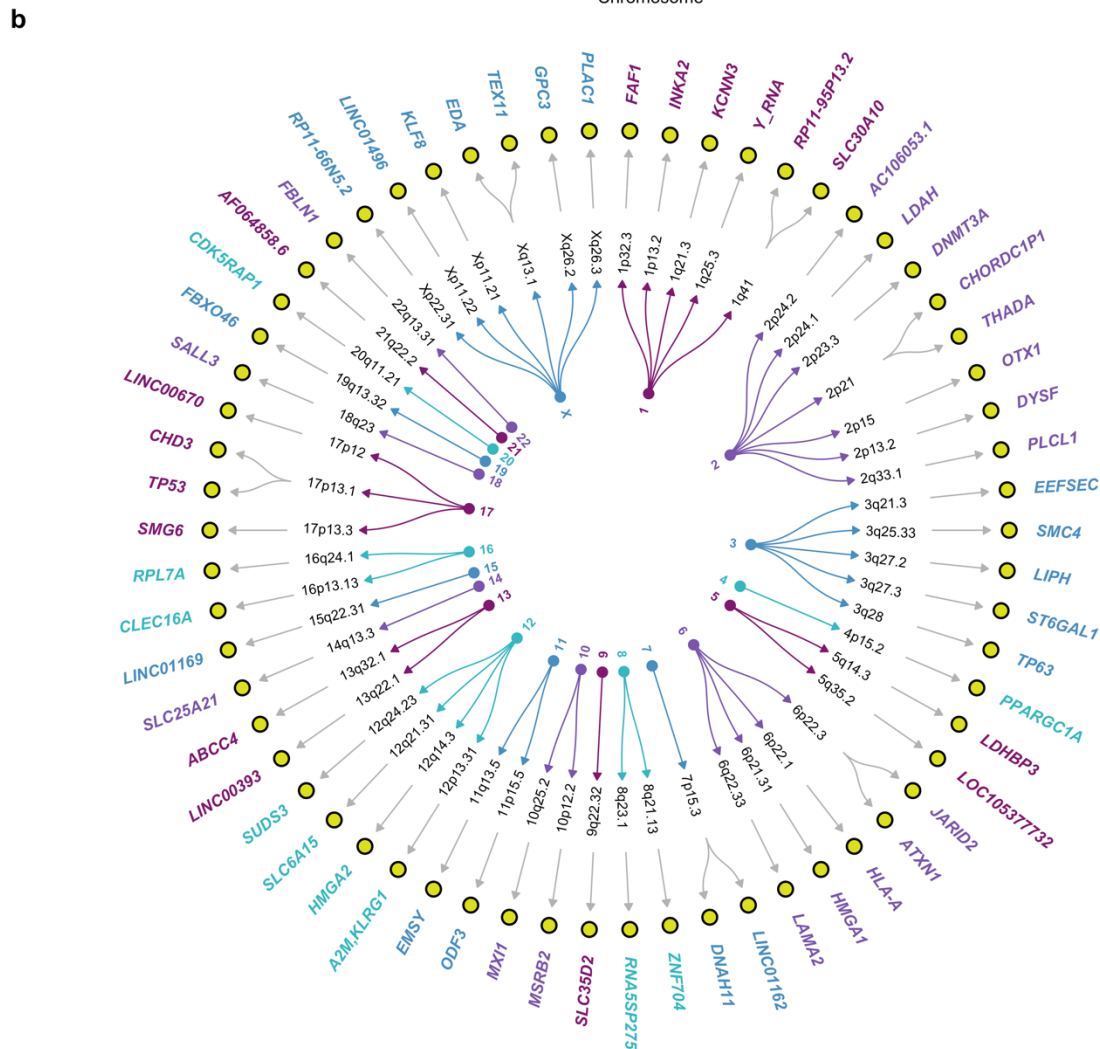
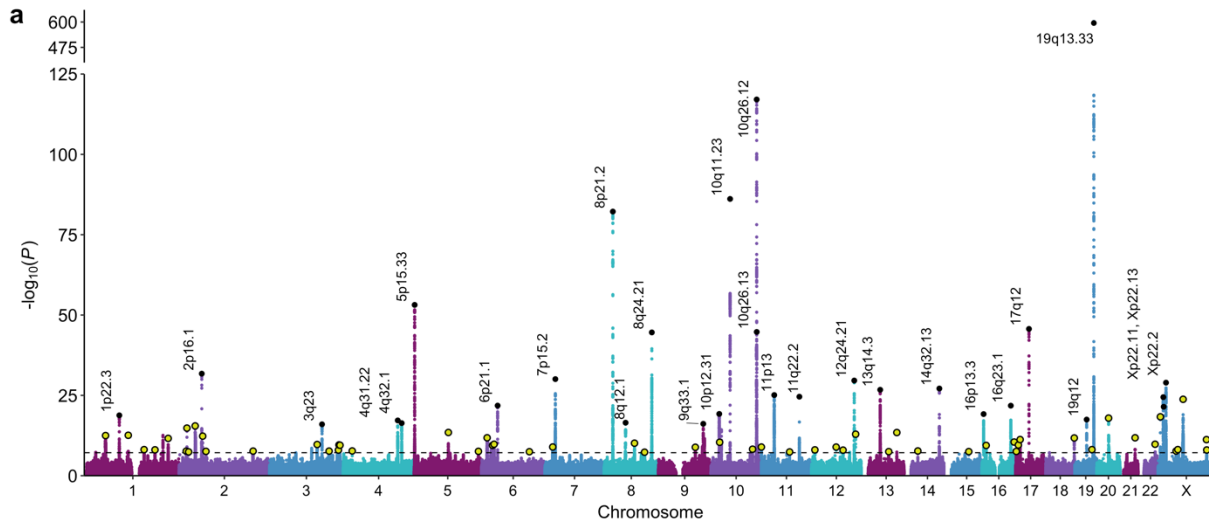
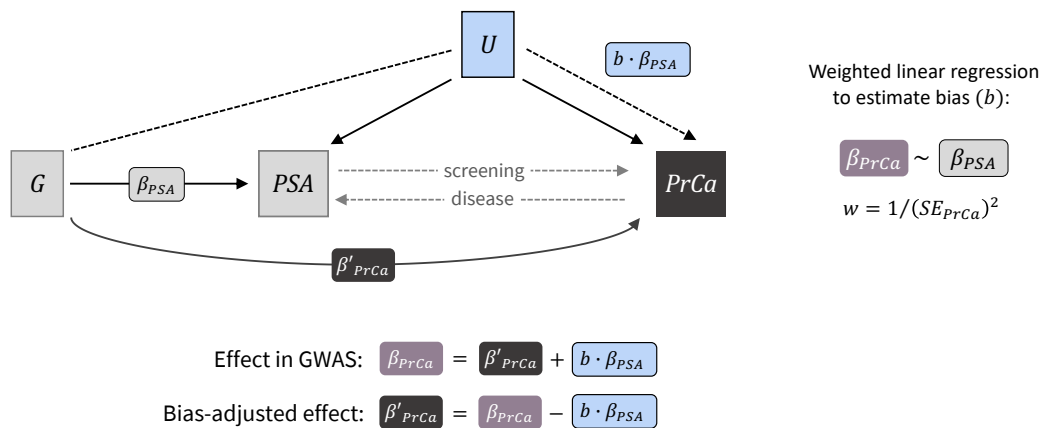
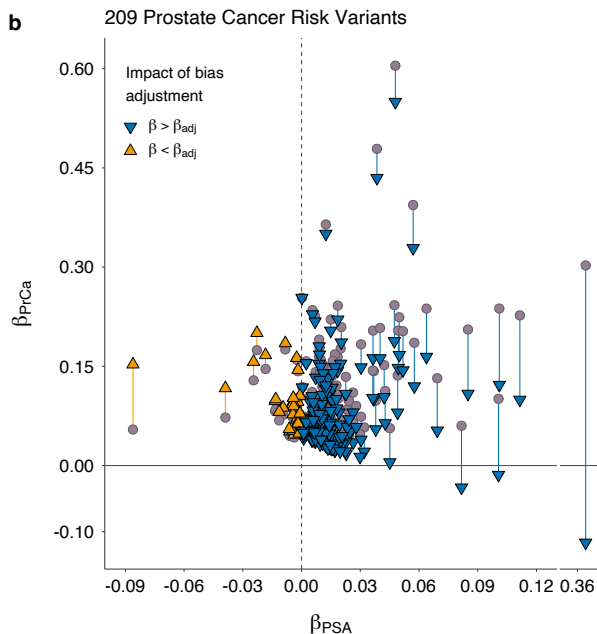


Fig. 3: Influence of PSA-related index event bias on prostate cancer GWAS. **a**, Conceptual diagram depicts how selection on PSA levels induces an association between genetic variant G and U , a composite confounder that captures polygenic and non-genetic factors. This selection induces an association with prostate cancer (PrCa) via path $G - U \rightarrow$ PrCa, in addition to the direct $G \rightarrow$ PrCa effects. Bi-directional dotted lines show that PSA is not only a disease biomarker, but also influences screening behavior and the likelihood of prostate cancer detection. **b-c**, The impact of bias correction is shown for 209 prostate cancer risk variants. Independent risk variants were selected from the PRACTICAL GWAS meta-analysis (85,554 cases and 91,972 controls of European ancestry) by Conti et al.³² using linkage disequilibrium (LD) clumping ($LD r^2 < 0.01, P < 5 \times 10^{-8}$). For each variant, associations with PSA (β_{PSA}) are based on an inverse-variance-weighted fixed-effects meta-analysis in men of European ancestry ($n=85,824$). **b**, GWAS effect sizes for prostate cancer (β_{PrCa}) are aligned to the risk-increasing allele. Bias-adjusted effect sizes (β_{adj}) are denoted by triangles **c**, Two-sided GWAS p-values for prostate cancer (P_{PrCa}) were derived from an inverse-variance-weighted fixed-effects meta-analysis. Two-sided bias-adjusted p-values (P_{adj}), denoted by triangles, were calculated from a chi-squared test statistic based on β_{adj} and corresponding standard errors. Genome-wide significance threshold ($P < 5 \times 10^{-8}$) is indicated by the dotted line.

a



b



c

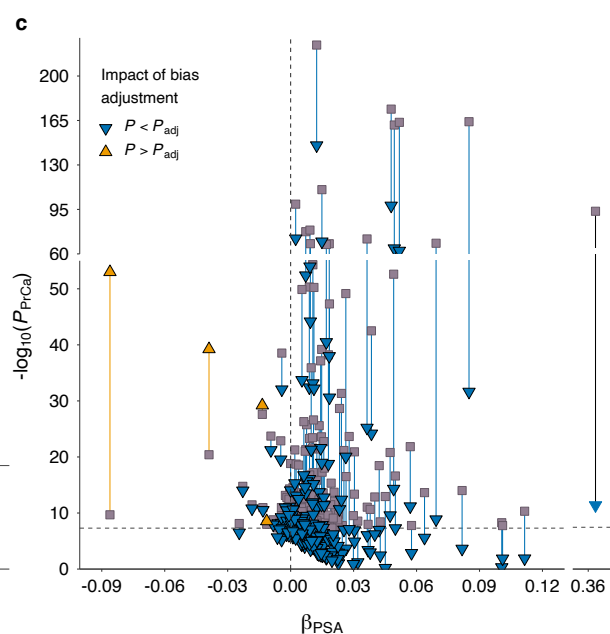


Fig. 4: Validation of the polygenic score for PSA (PGS_{PSA}) in two cancer prevention trials. Performance of PGS_{PSA} was evaluated in the Prostate Cancer Prevention Trial (PCPT) and Selenium and Vitamin E Cancer Prevention Trial (SELECT). Violin plots show the distribution of baseline log(PSA) within quantiles of PGS_{PSA}, comprised of 1,058,173 and 1,071,278 variants in **a**, PCPT and **b**, SELECT. Box plots extend from the 25th to the 75th percentiles, with a trend line connecting the median value within each age stratum. Two-sided p-values are derived from linear regression models for the effect of a quantile increase in PGS_{PSA} on log(PSA). **c-d**, Crossbar plots show the effect estimates (β) and corresponding 95% intervals per standard deviation (SD) increase in the standardized PGS_{PSA} on baseline log(PSA) **c**, PCPT and **d**, SELECT. Ancestry-stratified and pooled, multi-ancestry estimates are presented. Two-sided p-values based on linear regression models are annotated. **e-f**. Comparison of distributions for PSA and genetically adjusted PSA (PSA^G), with the horizontal line at 4 ng/mL, a commonly used threshold for further diagnostic testing. Box plots show the median value with lower and upper hinges corresponding to the 25th to the 75th percentiles, or first and third quartiles. Whiskers extend as a multiple of the inter-quartile range (IQR*1.5). Outlying values beyond the end of the whiskers are plotted individually.

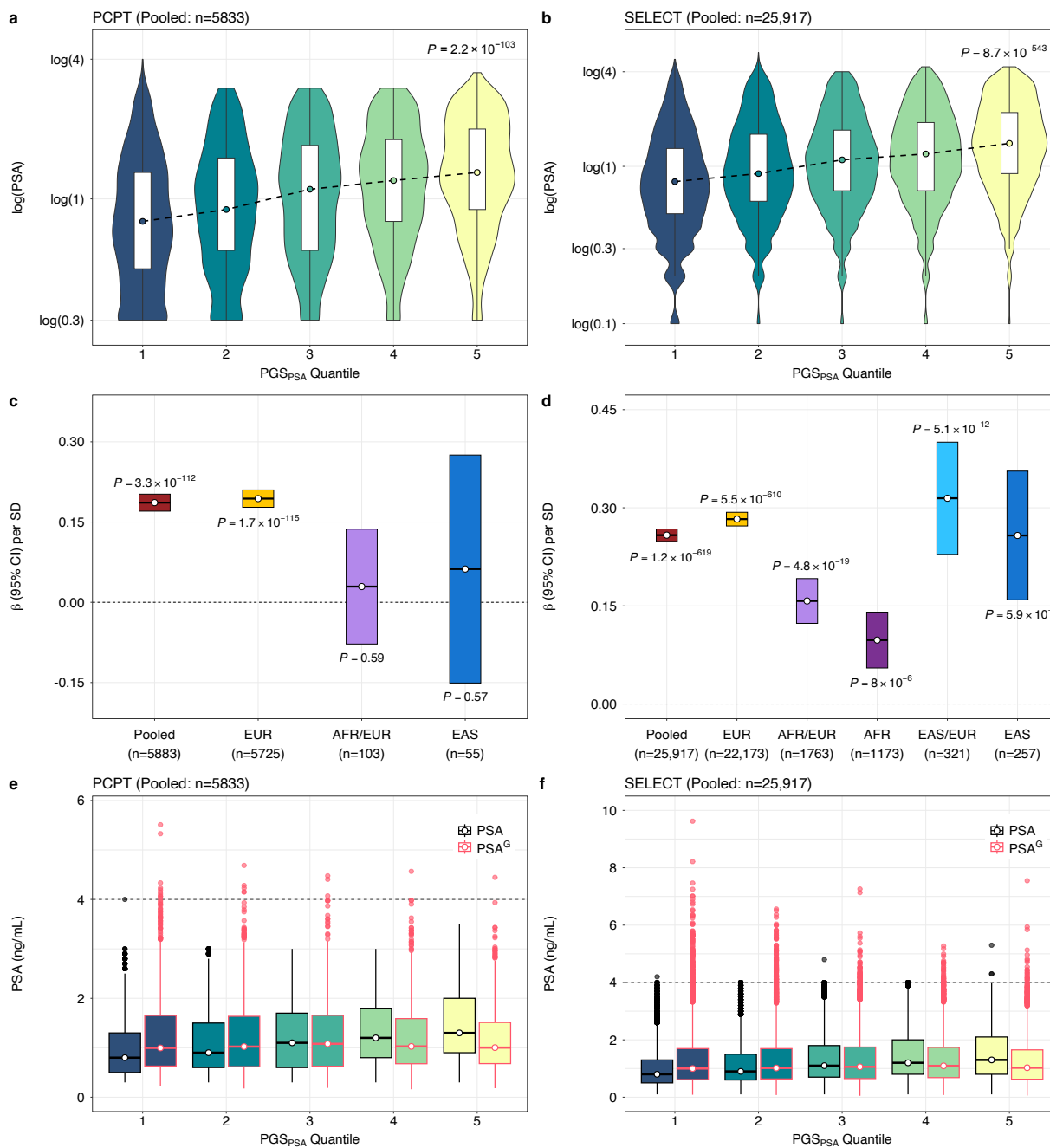


Fig. 5: Genetically adjusted PSA influences biopsy eligibility. Flow diagrams illustrate changes in PSA values after genetic adjustment for participants in the Genetic Epidemiology Research in Adult Health and Aging (GERA) cohort, and subsequent reclassification at PSA thresholds used to recommend prostate biopsy. Genetic adjustment was applied to the last pre-biopsy PSA value to obtain PSA^G. Analyses were performed separately in men of **a**, European and **b**, African ancestry. Size of the nodes and flows are proportional to the number of individuals in each category. Prostate cancer patients (cases) were stratified by Gleason score categories, where Gleason <7 represents potentially indolent disease. Gleason score is not applicable to men with a negative prostate biopsy (controls).

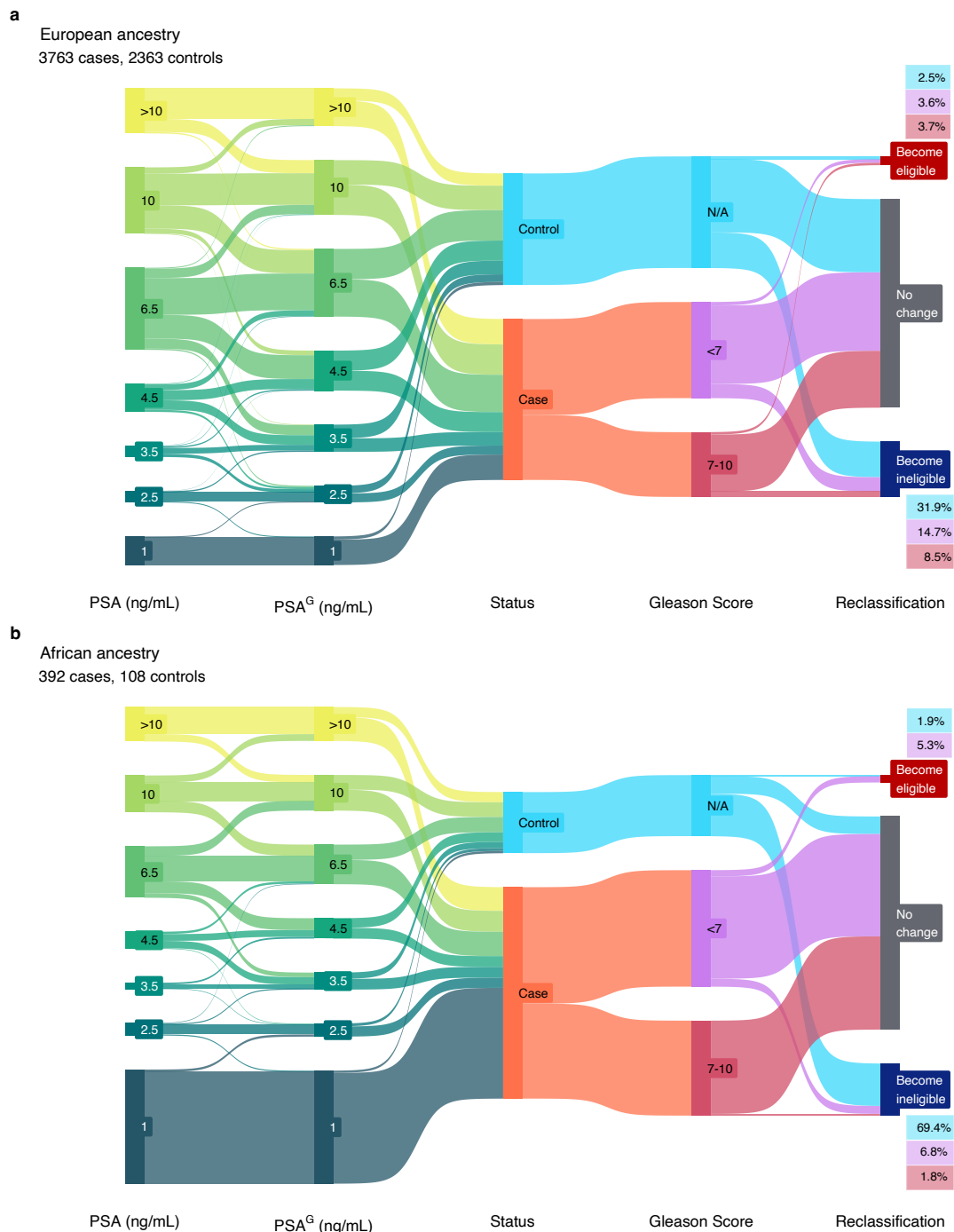
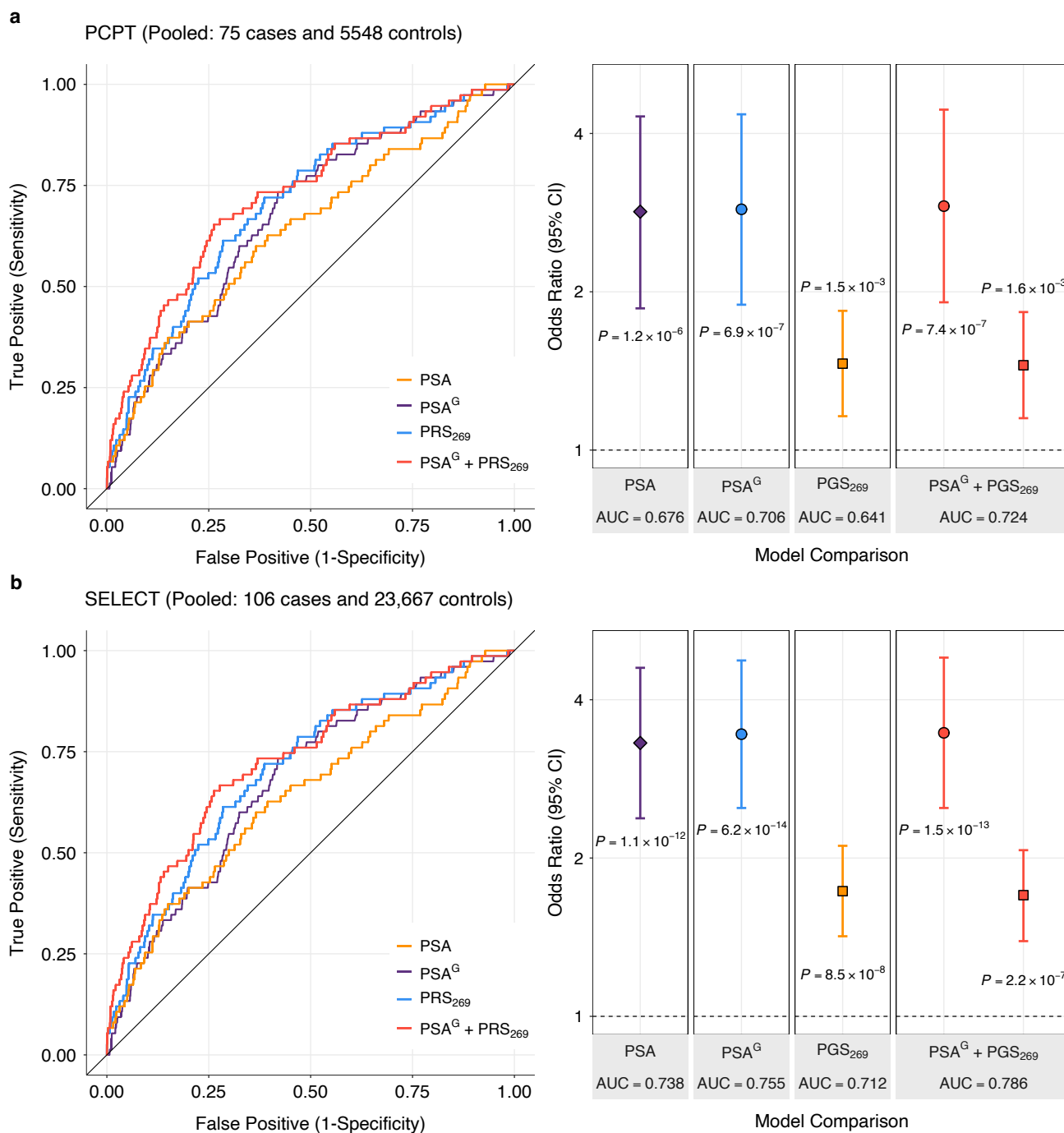


Fig. 6: Genetic associations with aggressive prostate cancer. Comparison of models for aggressive disease, defined as Gleason score ≥ 7 , PSA ≥ 10 ng/mL, T3-T4 stage, and/or distant or nodal metastases in the **a**, the Prostate Cancer Prevention Trial (PCPT) and **b**, Selenium and Vitamin E Cancer Prevention Trial (SELECT). The pooled study population includes all ancestry groups. Logistic regression models adjusted for baseline age, randomization arm, the top 10 population-specific genetic ancestry principal components, and proportions of African and East Asian genetic ancestry. Odds ratios (OR) and 95% confidence intervals were estimated per 1-unit increase in $\log(\text{PSA ng/mL})$ and $\log(\text{PSA}^G \text{ ng/mL})$, and per standard deviation (SD) increase in the prostate cancer genetic risk score (PGS₂₆₉) from Conti et al.³², which was standardized to achieve SD equal to 1. All p-values are two-sided. AUC is based on the full model with all covariates.



References

1. Lilja, H. A kallikrein-like serine protease in prostatic fluid cleaves the predominant seminal vesicle protein. *J Clin Invest* **76**, 1899-1903 (1985).
2. Balk, S.P., Ko, Y.J. & Bubley, G.J. Biology of prostate-specific antigen. *J Clin Oncol* **21**, 383-391 (2003).
3. Lilja, H., Ulmert, D. & Vickers, A.J. Prostate-specific antigen and prostate cancer: prediction, detection and monitoring. *Nat Rev Cancer* **8**, 268-278 (2008).
4. Pinsky, P.F., *et al.* Prostate volume and prostate-specific antigen levels in men enrolled in a large screening trial. *Urology* **68**, 352-356 (2006).
5. Lee, S.E., *et al.* Relationship of prostate-specific antigen and prostate volume in Korean men with biopsy-proven benign prostatic hyperplasia. *Urology* **71**, 395-398 (2008).
6. Grubb, R.L., 3rd, *et al.* Serum prostate-specific antigen hemodilution among obese men undergoing screening in the Prostate, Lung, Colorectal, and Ovarian Cancer Screening Trial. *Cancer Epidemiol Biomarkers Prev* **18**, 748-751 (2009).
7. Harrison, S., *et al.* Systematic review and meta-analysis of the associations between body mass index, prostate cancer, advanced prostate cancer, and prostate-specific antigen. *Cancer Causes Control* **31**, 431-449 (2020).
8. Thompson, I.M., *et al.* Assessing prostate cancer risk: results from the Prostate Cancer Prevention Trial. *J Natl Cancer Inst* **98**, 529-534 (2006).
9. Schroder, F.H., *et al.* Screening and prostate-cancer mortality in a randomized European study. *N Engl J Med* **360**, 1320-1328 (2009).
10. Telesca, D., Etzioni, R. & Gulati, R. Estimating lead time and overdiagnosis associated with PSA screening from prostate cancer incidence trends. *Biometrics* **64**, 10-19 (2008).
11. Welch, H.G. & Black, W.C. Overdiagnosis in cancer. *J Natl Cancer Inst* **102**, 605-613 (2010).
12. Vickers, A.J., *et al.* Empirical estimates of prostate cancer overdiagnosis by age and prostate-specific antigen. *BMC Med* **12**, 26 (2014).
13. Vickers, A.J., *et al.* Strategy for detection of prostate cancer based on relation between prostate specific antigen at age 40-55 and long term risk of metastasis: case-control study. *BMJ* **346**, f2023 (2013).
14. Kovac, E., *et al.* Association of Baseline Prostate-Specific Antigen Level With Long-term Diagnosis of Clinically Significant Prostate Cancer Among Patients Aged 55 to 60 Years: A Secondary Analysis of a Cohort in the Prostate, Lung, Colorectal, and Ovarian (PLCO) Cancer Screening Trial. *JAMA Netw Open* **3**, e1919284 (2020).
15. Tikkinen, K.A.O., *et al.* Prostate cancer screening with prostate-specific antigen (PSA) test: a clinical practice guideline. *BMJ* **362**, k3581 (2018).
16. Force, U.S.P.S.T., *et al.* Screening for Prostate Cancer: US Preventive Services Task Force Recommendation Statement. *JAMA* **319**, 1901-1913 (2018).
17. Hoffmann, T.J., *et al.* Genome-wide association study of prostate-specific antigen levels identifies novel loci independent of prostate cancer. *Nat Commun* **8**, 14248 (2017).
18. Bansal, A., *et al.* Heritability of prostate-specific antigen and relationship with zonal prostate volumes in aging twins. *J Clin Endocrinol Metab* **85**, 1272-1276 (2000).
19. Gudmundsson, J., *et al.* Genetic correction of PSA values using sequence variants associated with PSA levels. *Sci Transl Med* **2**, 62ra92 (2010).
20. Benafif, S., Kote-Jarai, Z., Eeles, R.A. & Consortium, P. A Review of Prostate Cancer Genome-Wide Association Studies (GWAS). *Cancer Epidemiol Biomarkers Prev* **27**, 845-857 (2018).
21. Wiklund, F., *et al.* Association of reported prostate cancer risk alleles with PSA levels among men without a diagnosis of prostate cancer. *Prostate* **69**, 419-427 (2009).
22. Kim, S., Shin, C. & Jee, S.H. Genetic variants at 1q32.1, 10q11.2 and 19q13.41 are associated with prostate-specific antigen for prostate cancer screening in two Korean population-based cohort studies. *Gene* **556**, 199-205 (2015).
23. Yang, J., Lee, S.H., Goddard, M.E. & Visscher, P.M. GCTA: a tool for genome-wide complex trait analysis. *Am J Hum Genet* **88**, 76-82 (2011).
24. Speed, D., Holmes, J. & Balding, D.J. Evaluating and improving heritability models using summary statistics. *Nat Genet* **52**, 458-462 (2020).
25. Bulik-Sullivan, B.K., *et al.* LD Score regression distinguishes confounding from polygenicity in genome-wide association studies. *Nat Genet* **47**, 291-295 (2015).
26. Ning, Z., Pawitan, Y. & Shen, X. High-definition likelihood inference of genetic correlations across human complex traits. *Nat Genet* **52**, 859-864 (2020).

27. Magi, R., *et al.* Trans-ethnic meta-regression of genome-wide association studies accounting for ancestry increases power for discovery and improves fine-mapping resolution. *Hum Mol Genet* **26**, 3639-3650 (2017).
28. Rentzsch, P., Schubach, M., Shendure, J. & Kircher, M. CADD-Splice-improving genome-wide variant effect prediction using deep learning-derived splice scores. *Genome Med* **13**, 31 (2021).
29. Mao, Y.Q. & Houry, W.A. The Role of Pontin and Reptin in Cellular Physiology and Cancer Etiology. *Front Mol Biosci* **4**, 58 (2017).
30. Egydio de Carvalho, C., *et al.* Molecular cloning and characterization of a complementary DNA encoding sperm tail protein SHIPPO 1. *Biol Reprod* **66**, 785-795 (2002).
31. Currall, B.B., *et al.* Loss of LDAH associated with prostate cancer and hearing loss. *Hum Mol Genet* **27**, 4194-4203 (2018).
32. Conti, D.V., *et al.* Trans-ancestry genome-wide association meta-analysis of prostate cancer identifies new susceptibility loci and informs genetic risk prediction. *Nat Genet* **53**, 65-75 (2021).
33. Dudbridge, F., *et al.* Adjustment for index event bias in genome-wide association studies of subsequent events. *Nat Commun* **10**, 1561 (2019).
34. Paternoster, L., Tilling, K. & Davey Smith, G. Genetic epidemiology and Mendelian randomization for informing disease therapeutics: Conceptual and methodological challenges. *PLoS Genet* **13**, e1006944 (2017).
35. Mahmoud, O., Dudbridge, F., Davey Smith, G., Munafo, M. & Tilling, K. A robust method for collider bias correction in conditional genome-wide association studies. *Nat Commun* **13**, 619 (2022).
36. Ruan, Y., *et al.* Improving polygenic prediction in ancestrally diverse populations. *Nat Genet* **54**, 573-580 (2022).
37. Lippman, S.M., *et al.* Effect of selenium and vitamin E on risk of prostate cancer and other cancers: the Selenium and Vitamin E Cancer Prevention Trial (SELECT). *JAMA* **301**, 39-51 (2009).
38. Kjaergaard, A.D., Bojesen, S.E., Nordestgaard, B.G., Johansen, J.S. & Smith, G.D. Biomarker de-Mendelization: principles, potentials and limitations of a strategy to improve biomarker prediction by reducing the component of variance explained by genotype. *bioRxiv*, 428276 (2018).
39. Holmes, M.V. & Davey Smith, G. Can Mendelian Randomization Shift into Reverse Gear? *Clin Chem* **65**, 363-366 (2019).
40. Enroth, S., Johansson, A., Enroth, S.B. & Gyllensten, U. Strong effects of genetic and lifestyle factors on biomarker variation and use of personalized cutoffs. *Nat Commun* **5**, 4684 (2014).
41. Yatsenko, A.N., *et al.* X-linked TEX11 mutations, meiotic arrest, and azoospermia in infertile men. *N Engl J Med* **372**, 2097-2107 (2015).
42. Astle, W.J., *et al.* The Allelic Landscape of Human Blood Cell Trait Variation and Links to Common Complex Disease. *Cell* **167**, 1415-1429 e1419 (2016).
43. Marouli, E., *et al.* Rare and low-frequency coding variants alter human adult height. *Nature* **542**, 186-190 (2017).
44. Bick, A.G., *et al.* Inherited causes of clonal haematopoiesis in 97,691 whole genomes. *Nature* **586**, 763-768 (2020).
45. Arbuckle, J.H. & Kristie, T.M. Epigenetic repression of herpes simplex virus infection by the nucleosome remodeler CHD3. *mBio* **5**, e01027-01013 (2014).
46. Shen, X., *et al.* Multivariate discovery and replication of five novel loci associated with Immunoglobulin G N-glycosylation. *Nat Commun* **8**, 447 (2017).
47. Wang, J.M., *et al.* KLRG1 negatively regulates natural killer cell functions through the Akt pathway in individuals with chronic hepatitis C virus infection. *J Virol* **87**, 11626-11636 (2013).
48. Kachuri, L., *et al.* The landscape of host genetic factors involved in immune response to common viral infections. *Genome Med* **12**, 93 (2020).
49. Rashkin, S.R., *et al.* Pan-cancer study detects genetic risk variants and shared genetic basis in two large cohorts. *Nat Commun* **11**, 4423 (2020).
50. Boyle, E.A., Li, Y.I. & Pritchard, J.K. An Expanded View of Complex Traits: From Polygenic to Omnigenic. *Cell* **169**, 1177-1186 (2017).
51. Di Giovannantonio, M., *et al.* Heritable genetic variants in key cancer genes link cancer risk with anthropometric traits. *J Med Genet* **58**, 392-399 (2021).
52. Filmus, J. & Capurro, M. The role of glypican-3 in the regulation of body size and cancer. *Cell Cycle* **7**, 2787-2790 (2008).
53. Moraru, A., *et al.* THADA Regulates the Organismal Balance between Energy Storage and Heat Production. *Dev Cell* **41**, 72-81 e76 (2017).
54. Vanbokhoven, H., Melino, G., Candi, E. & Declercq, W. p63, a story of mice and men. *J Invest Dermatol* **131**, 1196-1207 (2011).

55. Wang, H., *et al.* Transcriptional regulation of P63 on the apoptosis of male germ cells and three stages of spermatogenesis in mice. *Cell Death Dis* **9**, 76 (2018).
56. Neri, G., Gurrieri, F., Zanni, G. & Lin, A. Clinical and molecular aspects of the Simpson-Golabi-Behmel syndrome. *Am J Med Genet* **79**, 279-283 (1998).
57. Gulati, R., Inoue, L.Y., Gore, J.L., Katcher, J. & Etzioni, R. Individualized estimates of overdiagnosis in screen-detected prostate cancer. *J Natl Cancer Inst* **106**, djt367 (2014).
58. Catalona, W.J., *et al.* Use of the percentage of free prostate-specific antigen to enhance differentiation of prostate cancer from benign prostatic disease: a prospective multicenter clinical trial. *JAMA* **279**, 1542-1547 (1998).
59. Loeb, S., *et al.* The prostate health index selectively identifies clinically significant prostate cancer. *J Urol* **193**, 1163-1169 (2015).
60. Vickers, A.J. & Brewster, S.F. PSA Velocity and Doubling Time in Diagnosis and Prognosis of Prostate Cancer. *Br J Med Surg Urol* **5**, 162-168 (2012).

METHODS

Informed consent was obtained from all study participants. UK Biobank received ethics approval from the Research Ethics Committee (REC reference: 11/NW/0382) in accordance with the UK Biobank Ethics and Governance Framework. The research was conducted with approved access to UK Biobank data under application number 14105. The Vanderbilt Institutional Review Board approved the BioVU study. We used previously published PSA GWAS results from the GERA cohort by Hoffmann et al¹⁷. The original study was approved by the Kaiser Permanente Northern California Institutional Review Board and the University of California San Francisco Human Research Protection Program Committee on Human Research. The Malmö Diet and Cancer Study (MDCS) was approved by the local ethics committee. The PLCO study was approved by the institutional review board at each participating centre and the National Cancer Institute. The informed consent document signed by the PLCO study participants allows use of these data by investigators for discovery and hypothesis generation in the investigation of the genetic contributions to cancer and other adult diseases. Our study includes publicly posted genomic summary results from PLCO Atlas⁶¹. No IRB review is required for PLCO summary data use.

Study Populations and Phenotyping

Genome-wide association analyses of PSA levels were conducted using germline genetic data derived from DNA extracted from non-prostatic tissues (e.g., blood, buccal swabs). Analyses were restricted to cis-gender men, defined as individuals of biological male sex and self-reported male gender identity, who have never been diagnosed with prostate cancer. Men with a history of surgical resections of the prostate were excluded in studies for which this information was available. To reduce potential for reverse causation, analyses were limited to PSA values ≤ 10 ng/mL, which corresponds to low-risk prostate cancer based on the D'Amico prostate cancer risk classification system⁶², and PSA > 0.01 ng/mL, to ensure that individuals had a functional prostate not impacted by surgery or radiation.

The UK Biobank (UKB) is a population-based prospective cohort of over 500,000 individuals aged 40-69 years at enrollment in 2006-2010 with genetic and phenotypic data⁶³. Health-related outcomes were ascertained via individual record linkage to national cancer and mortality registries and hospital in-patient encounters. PSA values were abstracted from primary care records for a subset of participants linked to genetic data. Field code mappings used to identify PSA values included any serum PSA measure except for free PSA or ratio of free to total PSA (**Supplementary Table 25**).

The Kaiser Permanente Genetic Epidemiology Research on Adult Health and Aging (GERA) cohort used in this analysis has been previously described in Hoffmann et al¹⁷. Briefly, prostate cancer status was ascertained from the Kaiser Permanente Northern California Cancer Registry, the Kaiser Permanente Southern California Cancer Registry, or through review of clinical electronic health records. PSA levels were abstracted from Kaiser Permanente electronic health records from 1981 through 2015.

The Prostate, Lung, Colorectal and Ovarian (PLCO) Cancer Screening Trial is a completed randomized trial that enrolled approximately 155,000 participants between November 1993 and July 2001. PLCO was designed to determine the effects of screening on cancer-related mortality and secondary endpoints in men and women aged 55 to 74⁶⁴. Men randomized to the screening arm of the trial underwent annual screening with PSA for six years and digital rectal exam (DRE) for four years⁶⁴. These analyses were limited to men with a baseline PSA measurement who were randomized to the screening arm of the trial (N=29,524). Men taking finasteride at the time of PSA measurement were excluded from analysis.

The Vanderbilt University Medical Center BioVU resource is a synthetic derivative biobank linked to deidentified electronic health records⁶⁵. Analyses were based on PSA levels that were measured as part of routine clinical care.

The Malmö Diet and Cancer Study (MDCS) is a population-based prospective cohort study that recruited men and women aged between 44 and 74 years old who were living in Malmö, Sweden between 1991 and 1996 to investigate the impact of diet on cancer risk and mortality⁶⁶. These analyses included men from the MDCS who were not diagnosed with prostate cancer as of December 2014 and had available genotyping and baseline PSA measurements⁶⁶.

PCPT is a completed phase III randomized, double-blind, placebo-controlled trial of finasteride for prostate cancer prevention that began in 1993⁸. PCPT randomly assigned 18,880 men aged 55 years or older who had a normal DRE and PSA level ≤ 3 ng/mL to either finasteride or placebo. For men with multiple pre-randomization PSA values, the earliest value was selected. Cases included all histologically confirmed prostate cancers detected during the 7-year treatment period and tumors that were detected by the end-of-study prostate biopsy. Our analyses included the subset of PCPT participants that was genotyped on the Illumina Infinium Global Screening Array (GSAMD) 24v2-0 array.

SELECT is a completed phase III randomized, placebo-controlled trial of selenium (200 μ g/day from L-selenomethionine) and/or vitamin E (400 IU/day of all rac- α -tocopheryl acetate) supplementation for prostate cancer prevention³⁷. Between 2001 and 2004, 34,888 eligible participants were randomized. The minimum enrollment age was 50 years for African American men and 55 years for all other men³⁷. Additional eligibility requirements included no prior prostate cancer diagnosis, ≤ 4 ng/mL of PSA in serum, and a DRE not suspicious for cancer. For men who had multiple pre-randomization PSA values, the earliest value was selected. Our analyses included a subset of SELECT participants genotyped on the Illumina Infinium Global Screening Array (GSAMD) 24v2-0 array.

Quality Control and Genome-Wide Association Analyses

Standard genotyping and quality control (QC) procedures were implemented in each participating study. Prior to meta-analysis we applied variant-level QC filters that included low imputation quality ($INFO < 0.30$), $MAF < 0.005$, deviations from Hardy-Weinberg equilibrium ($P_{HWE} < 1 \times 10^{-5}$). Sample-level QC filtered based on discordant genetic sex and self-reported gender, call rate $\geq 97\%$, and removed one sample from each pair of first-degree relatives. GWAS phenotypes and adjustment covariates are reported in **Supplementary Table 26**. Genome-wide association analyses performed linear regression of $\log(\text{PSA})$ as the outcome, using age and genetic ancestry principal components (PC's) as the minimum set of covariates.

UK Biobank

Genotyping and imputation for the UK Biobank cohort have been previously described⁶³. Briefly, participants were genotyped on the UKB Affymetrix Axiom array (89%) or the UK BiLEVE array (11%) with imputation performed using the Haplotype Reference Consortium (HRC) and the merged UK10K and 1000 Genomes (1000G) phase 3 reference panels. Genetic ancestry principal components (PCs) were computed using fastPCA based on a set of 407,219 unrelated samples and 147,604 genetic markers⁶³. Association analyses in UKB were restricted to individuals of European ancestry based on self-report ("White") and after excluding samples with any of the first two genetic ancestry PC's outside of 5 standard deviations (SD) of the population mean, as previously described⁴⁹. We removed samples with discordant self-reported and genetic sex, as well as one sample from each pair of first-degree relatives identified using KING⁶⁷. Using a subset of genotyped autosomal variants with $(MAF) \geq 0.01$ and call rate $\geq 97\%$, we filtered samples with heterozygosity > 5 SD from the mean. For participants with multiple PSA measurements, the median value PSA was used. Sensitivity analyses were conducted comparing this approach to a GWAS of individual-specific random effects derived from fitting a linear mixed model to repeated $\log(\text{PSA})$ values.

Genetic Epidemiology Research on Adult Health and Aging (GERA)

Genotyping, imputation, and QC of the GERA cohort has been previously described^{17,68,69}. Briefly, all men were genotyped for over 650,00 SNPs on four race/ethnicity-specific Affymetrix Axiom arrays that were optimized for individuals who self-identified as non-Hispanic white, Latino, East Asian, and African American,

respectively^{68,69}. Genotype QC procedures and imputation for the original GERA cohort were performed on an array-wise basis, as previously described^{17,70}. Pre-phasing was done by SHAPEIT v2.5⁷¹ and imputation with IMPUTE2 v2.3.1⁷² using the 1000 Genomes Phase 3 release with 2504 samples. The top 10 genetic ancestry PC's from Eigenstrat v4.2, were included in the linear model as ancestry covariates⁷³. Analyses were conducted according to self-identified race/ethnicity groups. Residuals were computed from linear mixed models that were fit to repeated log(PSA) measures. This approach nearly identical to a long-term average, except it uses the median instead of the mean to handle any potential outlier PSA level values.

Prostate, Lung, Colorectal and Ovarian (PLCO) Atlas

Our study used GWAS summary statistics from the PLCO Atlas Project, a resource for multi-trait GWAS. Genotyping, QC, and imputation procedures for this resource are described by Machiela et al.⁶¹ The Atlas project combined genotyping data previously generated by high density arrays for 25,831 participants (OncoArray, Omni2.5 M, and OmniExpress) with a new round of genotyping using the Illumina Global Screening Array (GSA). For participants genotyped on multiple genotyping arrays (N = 1,192), data from only one array were retained, with the following prioritization: GSA > OncoArray > Omni2.5 M > OmniExpress (OmniX). Extensive quality control filtering was performed for subsequent imputation and association analyses. Iterative 80% and 95% sample- and variant-level call rate filters were applied to remove poorly genotyped samples and variants. Samples with greater than 20% estimated contamination based on VerifyBamID⁷⁴ were also removed. Samples with discordant self-reported gender and genetically inferred sex were identified based on X chromosome method-of-moments F coefficient from PLINK, using 0.5 as the threshold (F coefficients are close to 0.0 for males and 1.0 for females). Heterozygosity outliers were detected using absolute values from PLINK method-of-moments F coefficients >0.2.

Genetic ancestry was determined using GRAF⁷⁵ on a set of 10,000 pre-selected fingerprinting variants. Participants were assigned to 9 ancestral groups: "African", "African American", "East Asian", "European", "Hispanic1", "Hispanic2", "Other", "Other Asian", and "South Asian". Hispanic1 included individuals of Dominican or Puerto Rican ancestry whereas Hispanic2 included individuals of Mexican or Latin American ancestry. For parsimony we merged "African" and "African American" into a "African American (Combined)" and "East Asian" and "Other Asian" into a "East Asian (Combined)". Imputation was performed using the TOPMed 5b reference panel, which is accessible via the TOPMed Imputation Server hosted on the Michigan Imputation Server. Prior to imputation, variants with MAF ≤ 0.01, missingness ≥ 0.05, and Hardy Weinberg deviations ($P_{HWE} \leq 1 \times 10^{-6}$) were removed. Genotyped data were aligned to reference datasets using a community-recommended script (HRC-1000G-check-bim.pl from <https://www.well.ox.ac.uk/~wrayner/tools/>) that was modified to support the TOPMed 5b reference panel using a pre-existing test imputation with 1000 Genomes subjects. Pre-phasing using phased reference data from TOPMed release 5b was conducted using EAGLE 2.4⁷⁶. Imputation was conducted against the same reference panel using minimac4. GWAS was based on the first PSA value for each PLCO participant.

BioVU

Participants were identified using Vanderbilt University Medical Center's (VUMC) BioVU resource, a DNA biobank comprising ~270,000 individuals and linked to a de-identified electronic health record (EHR)⁶⁵. All participants (n=8,074) were genotyped on Illumina's Expanded Multi-Ethnic Genotyping Array (MEGA^{EX}) platform. Genetic ancestries were assigned by running principal component analysis using SNPRelate⁷⁷ on a set of pruned SNPs (Rsq < 0.5, MAF ≥ 0.1). Subjects were classified as being of European ancestry if their first two PCs were within 4 SDs of the median for the subjects reporting "White" as their race. Subjects were classified as being of African ancestry if their first two PCs were within 4 SDs of the median for subjects reporting their race as "Black". All quality control procedures were performed using PLINK version 1.90. We removed one randomly selected sample out of each pair of related individuals ($\pi\text{-hat} \geq 0.2$) identified using identity-by-descent. We excluded subjects with SNP missingness >3% or heterozygosity >5 SD from the mean. Prior to imputation, data were pre-processed using the HRC-1000G-check-bim.pl (from <http://www.well.ox.ac.uk/~wrayner/tools/>) and pre-phased using Eagle v2.4⁷⁶. Genetic data was imputed on

the Michigan Imputation Server using 1000 Genomes phase 3 version 5 as the reference panel. For men with multiple PSA measurements, the median PSA was used.

Malmö Diet and Cancer Study (MDCS)

Data from multiple batches of genotyping of 4069 MDCS participants using different Illumina Omni arrays were merged. For variants that appeared more than once under different names on the same Illumina array, those with the higher genotyping rate were retained. Indels, ambiguous palindromic (eg. A/T or C/G alleles) and multi-allelic variants were removed. Only SNPs that we could unambiguously map to 1000 Genomes phase 1 dataset were kept. Individuals with more than 10% missingness were removed. Next, SNPs with a missingness rate greater than 10% or deviation from Hardy-Weinberg equilibrium ($P_{HWE} < 0.001$) were removed. At this stage, the principal components of ancestry were computed. Individuals for whom the inferred sex based on X chromosome heterozygosity was not male, or for whom there were more than two genetic mismatches with 40 SNPs we had previously genotyped in these samples with targeted genotyping⁶⁶ were excluded.

To assess genetic ancestry, data were combined with data from HapMap phase 3 for variants present in all genotyping batches. These SNPs were further filtered to have less than 0.01% missingness and LD-pruned (--indep-parwise 50 5 0.05). SMARTPCA in EIGENSOFT (<https://github.com/chrchang/eigensoft>) was run on the resulting 18,299 SNPs to generate the top 10 genetic ancestry PC's. Analyses were restricted to individuals of European ancestry based on clustering with HapMap reference populations and exclusion of outliers with a Z-score on PC1 and PC2 greater than 5. Imputation was performed using the TOPMed 5b reference panel, which is accessible via the TOPMed Imputation Server hosted on the Michigan Imputation Server. Prior to imputation, the input file was aligned to the build37 reference genome on the basis of chromosome, position and alleles. A total of 847,133 SNPs that passed pre-imputation QC were uploaded to the imputation server. From the resulting imputed files, analyses were restricted to individuals without a prostate cancer diagnosis by December 31, 2014, with individual missingness less than 3%, a Z-score less than 5.0 for heterozygosity. Log(PSA) values were analyzed using robust linear regression with Tukey biweights. GWAS was performed using linear regression on the residuals were extracted from the fitted models.

Prostate Cancer Prevention Trial (PCPT) and Selenium and Vitamin E Cancer Prevention Trial (SELECT)

Participants from PCPT and SELECT were genotyped on the Illumina Infinium Global Screening Array (GSAMD) 24v2-0 array and underwent the same QC and imputation procedures. Genotyping calling and quality control were performed at the Center for Inherited Disease Research (CIDR) at Johns Hopkins After removal of samples that failed to produce valid output during initial processing and clustering, the completion rate was 0.9951 and 0.9959 in PCPT and SELECT, respectively. A two-stage filter by completion rate threshold of 0.8 for samples and 0.8 for variants, followed by 0.95 for samples and 0.95 for variants was performed. Samples with discordant self-reported gender and genetically inferred sex were identified based on X chromosome method-of-moments F coefficient from PLINK, using 0.5 as the threshold (F coefficients are close to 0.0 for males and 1.0 for females). Identity-by-descent (IBD) for all subject pairs were using PLINK and close (1st and 2nd degree) relatives were identified based on a threshold of 0.20. One randomly selected sample from pair of relatives was retained.

Ancestry was estimated using a set of LD-pruned markers and running SNPWEIGHTS⁷⁸ with the reference panel provided containing the following populations: European, West African, and East Asian, with a threshold of 0.8 used for imputed ancestry designation. Subjects were assigned to a single ancestry group if the ancestry score was equal to or above 0.80 for just one group. Individuals were assigned to an admixed cluster if their ancestry score was >0.20 and <0.80 for only one group (eg: ADMIXED_AFR where AFR=0.75, EUR=0.17, EAS=8). Intermediate ancestry clusters included individuals with ancestry scores matching those criteria in multiple groups: $0.20 < \text{AFR_EUR} < 0.80$ (eg: AFR=0.65, EUR=0.33) and $0.20 < \text{EAS_EUR} < 0.80$ (eg: EUR=0.55, EAS=0.43). Autosomal heterozygosity was assessed using the method-of-moments F coefficient calculated within each ancestry cluster. Heterozygosity outliers were identified and excluded using a

threshold of 0.10. Principal components analysis was performed with SMARTPCA in EIGENSOFT (<https://github.com/chrchang/eigensoft>) on a set of LD-pruned markers after splitting by ancestry cluster, to resolve more detailed population substructure. Genetic ancestry PC's were not computed for small clusters ($n < 50$) or individuals who failed other QC filters. For validation of PGS_{PSA} in PCPT and SELECT we combined ADMIXED_AFR and AFR_EUR and treated this as a single group with admixed AFR and EUR ancestry proportions (AFR/EUR). ADMIXED_EAS and EAS_EUR were also combined into a single cluster with admixed EAS and EUR ancestry (EAS/EUR).

To prepare genotype data for imputation with the TOPMed 5b reference panel, variants with $MAF < 0.001$, call rate $< 98\%$, or evidence of deviation from Hardy-Weinberg equilibrium ($P_{HWE} < 10^{-6}$) were removed. After these QC step, a total of 474,046 variants remained for PCPT and 491,015 variants were retained for SELECT. Prior to submitting the data to the TOPMed Imputation Server, files were pre-processed using the check-bim.pl script (<http://www.well.ox.ac.uk/~wrayner/tools/>). Next, chromosomal positions were lifted over from GRCh37/hg19 to GRCh38 and aligned against the TOPMed reference SNP list based on chromosome, position, and alleles to ensure that reference and alternate alleles were correct in the resulting VCF files.

Heritability of PSA Levels Attributed to Common Variants

Heritability of PSA levels was estimated using individual-level data and GWAS summary statistics. UKB participants with available PSA and genetic data were analyzed using Linkage Disequilibrium Adjusted Kinships (LDAK) v5.1²⁴ and GCTA v1.93²³, following the approach previously implemented in the GERA cohort¹⁷. Genetic relationship matrices were filtered to ensure that no pairwise relationships with kinship estimates > 0.05 remained. Heritability was estimated using common ($MAF \geq 0.01$) LD-pruned ($r^2 < 0.80$) variants with imputation INFO > 0.80 . We implemented the LDAK-Thin model using the recommended GRM settings (INFO > 0.95 , LD $r^2 < 0.98$ within 100 kb) and the same parameters as GCTA for comparison (LD $r^2 < 0.80$, INFO > 0.80). For both methods, sensitivity analyses were conducted using more stringent GRM settings (kinship = 0.025, genotyped variants).

Summary statistics from GWAS results based on the same set of UKB participants ($n = 26,491$) and from a European ancestry GWAS meta-analysis ($n = 85,824$) were analyzed using LDAK, LD score regression (LDSR)²⁵, and an extension of LDSR using a high-definition likelihood (HDL) approach²⁶. For LDSR we used the default panel comprised of variants available in HapMap3 with weights computed in 1000 Genomes v3 EUR individuals and in-house LD scores computed in UKB European ancestry participants⁴⁹. The baseline linkage disequilibrium (BLD)-LDAK model was fit using precomputed tagging files calculated in UKB GBR (white British) individuals for HapMap3 variants from the LDSR default panel. HDL analyses were conducted using the UKB-derived panel restricted to high-quality imputed HapMap3 variants²⁶. All GWAS summary statistics had sufficient overlap with the reference panels, not exceeding the 1% missingness threshold for HDL and 5% missingness threshold for LDAK and LDSR.

Genome-Wide Meta-Analysis

Each ancestral population was analyzed separately, and GWAS summary statistics were combined via meta-analysis (**Figure 1**). We first used METAL⁷⁹ to conduct an inverse-variance-weighted fixed-effects meta-analysis in each ancestry group and then meta-analyzed the ancestry-stratified results. Multi-ancestry meta-analysis results were processed using clumping to identify independent association signals by grouping variants based on linkage disequilibrium within specific windows. Clumps were formed around index variants with the lowest genome-wide significant ($P < 5 \times 10^{-8}$) meta-analysis p-value. All other variants with LD $r^2 > 0.01$ within a ± 10 Mb window were considered non-independent and assigned to that lead variant. Since over 90% of the meta-analysis consisted of individuals of European ancestry, clumping was performed using 1000 Genomes (1000G) Phase 3 EUR and UKB reference panels, which yielded concordant results. We confirmed that LD among the resulting lead variants did not exceed $r^2 = 0.05$ using a merged 1000G ALL reference panel.

We first examined heterogeneity in the multi-ancestry fixed-effects meta-analysis results using Cochran's Q statistic. To assess heterogeneity specifically due to ancestry we applied MR-MEGA²⁷, a meta-regression approach for aggregating GWAS results across diverse populations. Summary statistics from each GWAS were meta-analyzed using MR-MEGA without combining by ancestry first. The MR-MEGA analysis was performed across four axes of genetic variation derived from pairwise allele frequency differences, based on the recommendation for separating major global ancestry groups. Index variants from the MR-MEGA analysis were selected using the same clumping parameters as described above (LD $r^2 < 0.01$ within $\pm 10\text{Mb}$ window), based on the merged 1000G ALL reference panel. For each variant, we report two heterogeneity p-values: one that is correlated with ancestry and accounted for in the meta-regression ($P_{\text{Het-Anc}}$) and the residual heterogeneity that is not due to population genetic differences ($P_{\text{Het-Res}}$).

PSA Genetic Score (PGS_{PSA}) Development and Validation

We implemented two strategies for generating a genetic score for PSA levels. In the first approach, we selected 128 variants that were genome-wide significant ($P < 5 \times 10^{-8}$) in the multi-ancestry meta-analysis and were independent (LD $r^2 < 0.01$ within $\pm 10\text{Mb}$ window) in 1000G EUR and (LD $r^2 < 0.05$) 1000G ALL populations (PGS₁₂₈). Each variant in PGS₁₂₈ was weighted by the meta-analysis effect size estimated using METAL. As an alternative strategy to clumping and thresholding, we fit a genome-wide score using the PRS-CSx algorithm³⁶, which takes GWAS summary statistics from each ancestry group as inputs and estimates posterior SNP effect sizes under coupled continuous shrinkage priors across populations (PGS_{CSx}). Analyses were conducted using pre-computed population-specific LD reference panels from the UKB, which included 1,287,078 HapMap3 variants that are available in both the UKB and 1000 Genomes Phase 3.

We calculated a single trans-ancestry PGS that can be applied to all participants in the target cohort, rather than optimizing a PGS within each ancestry group. This approach is more robust to differences in genetic ancestry assignments across studies and does not require separate testing and validation datasets for parameter tuning each ancestry group³⁶. To facilitate this type of analysis, PRS-CSx provides a --meta option that integrates population-specific posterior SNP effects using an inverse-variance-weighted meta-analysis in the Gibbs sampler³⁶. The global shrinkage parameter was set to $\phi = 0.0001$. PRS-CSx was run on the intersection of variants that were in the LD reference panel and had imputation quality (INFO > 0.90), resulting in 1,058,163 variants in PCPT and 1,071,268 variants in SELECT. Since PRS-CSx only considers autosomes, chrX variants that were included in PGS₁₂₈ were added to PGS_{CSx} separately, when output files from each chromosome produced by the PLINK --score command were concatenated.

The predictive performance of PGS_{CSx} and PGS₁₂₈ was evaluated in two independent cancer prevention trials that were not included in the meta-analysis: PCPT and SELECT. Analyses were conducted in the pooled sample for each cohort, which included individuals of all ancestries who passed quality control filters (**see Supplementary Note**). Ancestry-stratified analyses were conducted for clusters with $n > 50$ with available genetic ancestry PC's. Ancestry scores were computed with SNPWEIGHTS⁷⁸. Individuals with ancestry scores ≥ 0.80 for a single group were assigned to clusters for predominantly European (EUR), West African (AFR) and East Asian (EAS) ancestry. Admixed individuals with intermediate ancestry scores for at least one group were assigned to separate clusters: $0.20 < \text{EUR/AFR} < 0.80$ or $0.20 < \text{EUR/EAS} < 0.80$. Pooled analyses were adjusted for 10 within-cluster PC's and global ancestry proportions (AFR, EAS).

Index Event Bias Analysis

Index event bias occurs when individuals are selected based on the occurrence of an event or specific criterion. This is analogous to the direct dependence of one phenotype on another, as in the commonly used example of cancer survival³⁴. Due to unmeasured confounding, this dependence can induce correlations between previously independent risk factors among those selected^{33,34}. Genetic effects on prostate cancer can be viewed as conditional on PSA levels, since elevated PSA typically triggers diagnostic investigation. Genetic factors resulting in higher constitutive PSA levels may also increase the likelihood of prostate cancer detection due to more frequent testing (**Figure 4**). This selection mechanism could bias prostate cancer

GWAS associations by capturing both direct genetic effects on disease risk and selection-induced PSA signals. In the GWAS setting, methods using summary statistics have been developed to estimate and correct for this bias^{33,35}. Although typically derived assuming a binary selection trait, these methods are still applicable to selection or adjustment based on quantitative phenotypes³³. In this study, we conceptualized PSA variation as the selection trait and prostate cancer incidence as the outcome trait (**Figure 4**).

We applied the method described in Dudbridge et al.³³, which tests for index event bias and estimates the corresponding correction factor (b) by regressing genetic effects on the selection trait (PSA) against their effects on the subsequent trait (prostate cancer), with inverse variance weights: $w = 1/(SE_{PrCa})^2$. Summary statistics for prostate cancer were obtained from the most recent prostate cancer GWAS from the PRACTICAL consortium³². Sensitivity analyses were performed using SlopeHunter³⁵, an extension of the Dudbridge approach that allows for direct genetic effects on the index trait and subsequent trait to be correlated. For both methods, analyses were conducted using relevant summary statistics and 127,906 variants pruned at the recommended threshold³³ (LD $r^2 < 0.10$ in 250 kb windows) with MAF ≥ 0.05 in the 1000G EUR reference panel. After merging the pruned 1000G variants with each set of summary statistics, variants with large effects, ($|\beta| > 0.20$) on either log(PSA) or prostate cancer, were excluded. The resulting estimate (b), adjusted regression dilution using the SIMEX algorithm, was used as a correction factor to recover unbiased genetic effects for each variant: $\beta'_{PrCa} = \beta_{PrCa} - b * \beta_{PSA}$, where β_{PSA} is the per-allele effect on log(PSA), and β_{PrCa} is the log(OR) for prostate cancer.

The impact of the bias correction was assessed in three ways. First, genome-wide significant prostate cancer index variants were selected from the European ancestry PRACTICAL GWAS meta-analysis (85,554 cases and 91,972 controls) using clumping (LD $r^2 < 0.01$ within 10 Mb)³². We tabulated the number of variants that remained associated at $P < 5 \times 10^{-8}$ after bias correction. Next, we fit genetic scores for PSA and prostate cancer in men of European ancestry in UKB who were not included in the PSA or prostate cancer GWAS (11,568 prostate cancer cases and 152,884 controls). We compared the correlation between the PGS for PSA (PGS_{PSA}), comprised of 128 lead variants, and the 269-variant prostate cancer risk score fit with original risk allele weights (PGS₂₆₉) and with weights corrected for index event bias (PGS₂₆₉^{adj}). To allow adjustment for genetic ancestry PCs and genotyping array, associations between the two scores were estimated using linear regression models. Next, we examined associations for each genetic score (PGS₂₆₉, PGS₂₆₉^{adj}, PGS₂₆₉^{adj-S}) with prostate cancer in a subset of GERA participants who underwent a biopsy. Since GERA controls were included in the PSA GWAS meta-analysis, AUC estimates and corresponding bootstrapped 95% confidence intervals were obtained using 10-fold cross-validation. We also examined PGS associations with Gleason score, a marker of disease aggressiveness, which was not available in the UK Biobank. Multinomial logistic regression models with Gleason score ≤ 6 (reference), 7, and ≥ 8 as the outcome were fit for each score in 4584 cases from the GERA cohort.

Application of Genetically Adjusted PSA for Biopsy Referral and Prostate Cancer Detection

Genetically corrected PSA values were calculated for individual i as follows^{17,19}:

$$(1) \quad PSA_i^G = \frac{PSA_i}{a_i}$$

where a_i is a personalized adjustment factor derived from PGS_{PSA}. Since genetic effects were estimated for log(PSA), a_i for correcting PSA in ng/mL was derived as:

$$(2) \quad a_i = \frac{\exp(PGS_i)}{\overline{\exp(PGS)}}$$

$\overline{\exp(PGS)}$ can be estimated in controls without prostate cancer or obtained from an external control population^{17,19}. We see that $a_i > 1$ when an individual has a higher multiplicative increase in PSA than the sample average

due to their genetic profile, resulting in a lower genetically adjusted PSA compared to the observed value ($PSA_i^G < PSA_i$).

We evaluated the potential utility of PGS_{PSA} in two clinical contexts. First, we quantified the impact of using PSA_i^G on biopsy referrals by examining reclassification at age-specific PSA thresholds used in the Kaiser Permanente health system. Analyses were conducted in GERA participants with information on biopsy date and outcome, comprised of prostate cancer cases not included in the PSA GWAS and controls that were part of the PSA GWAS. To use the same normalization factor for both cases and controls while mitigating bias due to control overlap with the PSA discovery GWAS, a_i for GERA participants was calculated by substituting \overline{PGS} from out-of-sample UK Biobank controls ($n=152,884$). Upward classification resulting in biopsy eligibility occurred when $PSA_i^G > PSA_i \cap PSA_i^G > ref$, where ref was the biopsy referral threshold. Downward classification resulting in biopsy ineligibility was defined as: $PSA_i^G < PSA_i \cap PSA_i^G < ref$. Net reclassification (NR) was summarized separately for cases and controls:

$$NR_{\text{case}} = P(\text{up}|\text{case}) - P(\text{down}|\text{case})$$

$$NR_{\text{control}} = P(\text{down}|\text{control}) - P(\text{up}|\text{control})$$

This is equivalent to tabulating the proportion of individuals in each biopsy eligibility category:

$$NR_{\text{case}} = \left(\frac{n_{\text{eligible}}}{n_{\text{case}}} \right) - \left(\frac{n_{\text{ineligible}}}{n_{\text{case}}} \right)$$

$$NR_{\text{control}} = \left(\frac{n_{\text{ineligible}}}{n_{\text{control}}} \right) - \left(\frac{n_{\text{eligible}}}{n_{\text{control}}} \right)$$

For each NR proportion, 95% confidence intervals were obtained using the normal approximation:

$$NR \pm 1.96 \times \sqrt{\frac{|NR| \times (1 - |NR|)}{n}}$$

Next, we assessed the performance of risk prediction models for prostate cancer overall, aggressive prostate cancer, and non-aggressive prostate cancer in PCPT and SELECT. Since both studies were excluded from the PSA GWAS meta-analysis, a_i and PSA_i^G for PCPT and SELECT were calculated using \overline{PGS} observed in each respective study. Consistent with the PGS_{PSA} validation analysis, pooled analyses included individuals of all ancestries who passed quality control filters. To facilitate ancestry-stratified analyses in SELECT, especially for aggressive disease, we combined AFR and AFR/EUR clusters into a single group (AFR pooled) and similarly pooled EAS and EAS/EUR (EAS pooled). Aggressive prostate cancer was defined as Gleason score ≥ 7 , PSA ≥ 10 ng/mL, T3-T4 stage, and/or distant or nodal metastases. We compared AUC estimates for logistic regression models using the following predictors, alone and in combination: baseline PSA, genetically adjusted baseline PSA (PSA_i^G) PGS_{PSA} , prostate cancer risk score with original weights (PGS_{269})³² and weights corrected for index event bias (PGS_{269}^{adj}).

DATA AVAILABILITY

UK Biobank data are publicly available by request from <https://www.ukbiobank.ac.uk>. To maintain individuals' privacy, data on the GERA cohort are available by application to the Kaiser Permanente Research Bank (researchbank.kaiserpermanente.org). All PLCO genotype data is available in dbGaP18 under accession number phs001286.v2.p2 (<https://identifiers.org/dbgap:phs001286.v2.p2>). Companion phenotype data can be requested through the NCI Cancer Data Access System (CDAS) (<https://cdas.cancer.gov/plco/>). GWAS summary statistics are available directly from the PLCO Atlas GWAS Explorer website (<https://exploregwas.cancer.gov/plco-atlas/>) as well as accessed directly through API access (<https://exploregwas.cancer.gov/plco-atlas/#/api-access>). Genome-wide summary statistics for the PSA multi-ancestry meta-analysis and ancestry-stratified summary statistics for the development of the genome-wide PSA polygenic score are available from: <https://doi.org/10.5281/zenodo.7460134>. Scoring files for fitting PSA polygenic scores are available from the PGS Catalog: www.pgscatalog.org/score/PGS003378/ and www.pgscatalog.org/score/PGS003379/

CODE AVAILABILITY

Genome-wide association analyses were conducted using PLINK 2.0 version a3LM (<https://www.cog-genomics.org/plink/2.0/>). Fixed-effects inverse-variance-weighted meta-analysis was performed with METAL using SCHEME STDERR (https://genome.sph.umich.edu/wiki/METAL_Documentation). Weights for the genome-wide polygenic score for PSA were estimated using PRS-CSx (<https://github.com/getian107/PRScsx>). Scripts for fitting polygenic scores, performing the index event bias analysis, and calculating genetically adjusted PSA values are available at: https://github.com/lkachuri/precision_PSA

Methods References

8. Thompson, I.M., *et al.* Assessing prostate cancer risk: results from the Prostate Cancer Prevention Trial. *J Natl Cancer Inst* **98**, 529-534 (2006).
17. Hoffmann, T.J., *et al.* Genome-wide association study of prostate-specific antigen levels identifies novel loci independent of prostate cancer. *Nat Commun* **8**, 14248 (2017).
19. Gudmundsson, J., *et al.* Genetic correction of PSA values using sequence variants associated with PSA levels. *Sci Transl Med* **2**, 62ra92 (2010).
23. Yang, J., Lee, S.H., Goddard, M.E. & Visscher, P.M. GCTA: a tool for genome-wide complex trait analysis. *Am J Hum Genet* **88**, 76-82 (2011).
24. Speed, D., Holmes, J. & Balding, D.J. Evaluating and improving heritability models using summary statistics. *Nat Genet* **52**, 458-462 (2020).
25. Bulik-Sullivan, B.K., *et al.* LD Score regression distinguishes confounding from polygenicity in genome-wide association studies. *Nat Genet* **47**, 291-295 (2015).
26. Ning, Z., Pawitan, Y. & Shen, X. High-definition likelihood inference of genetic correlations across human complex traits. *Nat Genet* **52**, 859-864 (2020).
27. Magi, R., *et al.* Trans-ethnic meta-regression of genome-wide association studies accounting for ancestry increases power for discovery and improves fine-mapping resolution. *Hum Mol Genet* **26**, 3639-3650 (2017).
32. Conti, D.V., *et al.* Trans-ancestry genome-wide association meta-analysis of prostate cancer identifies new susceptibility loci and informs genetic risk prediction. *Nat Genet* **53**, 65-75 (2021).
33. Dudbridge, F., *et al.* Adjustment for index event bias in genome-wide association studies of subsequent events. *Nat Commun* **10**, 1561 (2019).
34. Paternoster, L., Tilling, K. & Davey Smith, G. Genetic epidemiology and Mendelian randomization for informing disease therapeutics: Conceptual and methodological challenges. *PLoS Genet* **13**, e1006944 (2017).
35. Mahmoud, O., Dudbridge, F., Davey Smith, G., Munafò, M. & Tilling, K. A robust method for collider bias correction in conditional genome-wide association studies. *Nat Commun* **13**, 619 (2022).
36. Ruan, Y., *et al.* Improving polygenic prediction in ancestrally diverse populations. *Nat Genet* **54**, 573-580 (2022).
37. Lippman, S.M., *et al.* Effect of selenium and vitamin E on risk of prostate cancer and other cancers: the Selenium and Vitamin E Cancer Prevention Trial (SELECT). *JAMA* **301**, 39-51 (2009).
49. Rashkin, S.R., *et al.* Pan-cancer study detects genetic risk variants and shared genetic basis in two large cohorts. *Nat Commun* **11**, 4423 (2020).
61. Machiela, M.J., *et al.* GWAS Explorer: an open-source tool to explore, visualize, and access GWAS summary statistics in the PLCO Atlas. *Sci Data* **10**, 25 (2023).
62. D'Amico, A.V. Risk-based management of prostate cancer. *N Engl J Med* **365**, 169-171 (2011).
63. Bycroft, C., *et al.* The UK Biobank resource with deep phenotyping and genomic data. *Nature* **562**, 203-209 (2018).
64. Andriole, G.L., *et al.* Mortality results from a randomized prostate-cancer screening trial. *N Engl J Med* **360**, 1310-1319 (2009).
65. Roden, D.M., *et al.* Development of a large-scale de-identified DNA biobank to enable personalized medicine. *Clin Pharmacol Ther* **84**, 362-369 (2008).
66. Klein, R.J., *et al.* Evaluation of multiple risk-associated single nucleotide polymorphisms versus prostate-specific antigen at baseline to predict prostate cancer in unscreened men. *Eur Urol* **61**, 471-477 (2012).
67. Manichaikul, A., *et al.* Robust relationship inference in genome-wide association studies. *Bioinformatics* **26**, 2867-2873 (2010).
68. Hoffmann, T.J., *et al.* Design and coverage of high throughput genotyping arrays optimized for individuals of East Asian, African American, and Latino race/ethnicity using imputation and a novel hybrid SNP selection algorithm. *Genomics* **98**, 422-430 (2011).
69. Hoffmann, T.J., *et al.* Next generation genome-wide association tool: design and coverage of a high-throughput European-optimized SNP array. *Genomics* **98**, 79-89 (2011).
70. Kvale, M.N., *et al.* Genotyping Informatics and Quality Control for 100,000 Subjects in the Genetic Epidemiology Research on Adult Health and Aging (GERA) Cohort. *Genetics* **200**, 1051-1060 (2015).
71. Delaneau, O., Marchini, J. & Zagury, J.F. A linear complexity phasing method for thousands of genomes. *Nat Methods* **9**, 179-181 (2011).

72. Howie, B., Fuchsberger, C., Stephens, M., Marchini, J. & Abecasis, G.R. Fast and accurate genotype imputation in genome-wide association studies through pre-phasing. *Nat Genet* **44**, 955-959 (2012).
73. Banda, Y., *et al.* Characterizing Race/Ethnicity and Genetic Ancestry for 100,000 Subjects in the Genetic Epidemiology Research on Adult Health and Aging (GERA) Cohort. *Genetics* **200**, 1285-1295 (2015).
74. Jun, G., *et al.* Detecting and estimating contamination of human DNA samples in sequencing and array-based genotype data. *Am J Hum Genet* **91**, 839-848 (2012).
75. Jin, Y., Schaffer, A.A., Sherry, S.T. & Feolo, M. Quickly identifying identical and closely related subjects in large databases using genotype data. *PLoS One* **12**, e0179106 (2017).
76. Loh, P.R., *et al.* Reference-based phasing using the Haplotype Reference Consortium panel. *Nat Genet* **48**, 1443-1448 (2016).
77. Zheng, X., *et al.* A high-performance computing toolset for relatedness and principal component analysis of SNP data. *Bioinformatics* **28**, 3326-3328 (2012).
78. Chen, C.Y., *et al.* Improved ancestry inference using weights from external reference panels. *Bioinformatics* **29**, 1399-1406 (2013).
79. Willer, C.J., Li, Y. & Abecasis, G.R. METAL: fast and efficient meta-analysis of genomewide association scans. *Bioinformatics* **26**, 2190-2191 (2010).